Bioaerosols in the atmosphere at two sites in Northern Europe in spring 2021: Outline of an experimental campaign

Sofiev, Mikhail

2022-11

þÿ S o f i e v , M , S o f i e v a , S , P a l a m a r c h u k , J , ` a u l i e n , I , K a d a n t s e v , E Fatahi , Y , Kouznetsov , R , Kuula , J , Noreikaite , A , Peltonen , M , Pihlajamäki , T T , Saarto , A , Salokas , J , Toiviainen , L , Tyuryakov , S , Sukiene , L , Asmi , E , Bamford , D H , Hyvärinen , A-P & Karppinen , A 2022 , ' Bioaerosols in the atmosphere at two sites in Northern Europe in spring 2021: Outline of an experimental campaign ' , Environmental Research , vol. 214 , no. Part 2 , 113798 . https://doi.org/10.1016/j.envres.2022.113798

http://hdl.handle.net/10138/347817
https://doi.org/10.1016/j.envres.2022.113798

Environmental Research 214 (2022) 113798

Contents lists available at ScienceDirect

Environmental Research

journal homepage: www.elsevier.com/locate/envres

Bioaerosols in the atmosphere at two sites in Northern Europe in spring 2021: Outline of an experimental campaign

Mikhail Sofiev [a,d,*], Svetlana Sofieva [a,b], Julia Palamarchuk [a], Ingrida Šaulienė [d], Evgeny Kadantsev [a], Nina Atanasova [a,b], Yalda Fatahi [a], Rostislav Kouznetsov [a], Joel Kuula [a], Auste Noreikaite [d], Martina Peltonen [a,b], Timo Pihlajamäki [a], Annika Saarto [c], Julija Svirskaite [a,b], Linnea Toiviainen [c], Svyatoslav Tyuryakov [a], Laura Šukienė [d], Eija Asmi [a], Dennis Bamford [b], Antti-Pekka Hyvärinen [a], Ari Karppinen [a]

[a] Finnish Meteorological Institute, Helsinki, Finland
[b] University of Helsinki, Helsinki, Finland
[c] University of Turku, Turku, Finland
[d] Vilnius University, Vilnius, Lithuania

ARTICLE INFO

Keywords:
Bioaerosols
Pollen
Fungal spores
Automatic pollen monitoring
Metagenomics
eDNA
3rd generation DNA sequencing

ABSTRACT

A coordinated observational and modelling campaign targeting biogenic aerosols in the air was performed during spring 2021 at two locations in Northern Europe: Helsinki (Finland) and Siauliai (Lithuania), approximately 500 km from each other in north-south direction. The campaign started on March 1, 2021 in Siauliai (12 March in Helsinki) and continued till mid-May in Siauliai (end of May in Helsinki), thus recording the transition of the atmospheric biogenic aerosols profile from winter to summer.

The observations included a variety of samplers working on different principles. The core of the program was based on 2- and 2.4–hourly sampling in Helsinki and Siauliai, respectively, with sticky slides (Hirst 24-h trap in Helsinki, Rapid-E slides in Siauliai). The slides were subsequently processed extracting the DNA from the collected aerosols, which was further sequenced using the 3-rd generation sequencing technology. The core sampling was accompanied with daily and daytime sampling using standard filter collectors. The hourly aerosol concentrations at the Helsinki monitoring site were obtained with a Poleno flow cytometer, which could recognize some of the aerosol types.

The sampling campaign was supported by numerical modelling. For every sample, SILAM model was applied to calculate its footprint and to predict anthropogenic and natural aerosol concentrations, at both observation sites.

The first results confirmed the feasibility of the DNA collection by the applied techniques: all but one delivered sufficient amount of DNA for the following analysis, in over 40% of the cases sufficient for direct DNA sequencing without the PCR step. A substantial variability of the DNA yield has been noticed, generally not following the diurnal variations of the total-aerosol concentrations, which themselves showed variability not related to daytime. An expected upward trend of the biological material amount towards summer was observed but the day-to-day variability was large.

The campaign DNA analysis produced the first high-resolution dataset of bioaerosol composition in the North-European spring. It also highlighted the deficiency of generic DNA databases in applications to atmospheric biota: about 40% of samples were not identified with standard bioinformatic methods.

1. Introduction

Primary biogenic aerosols (hereinafter, bioaerosols) are attracting increasing attention during recent years but existing information is scarce, owing to a wide variety of bioaerosol types, aerodynamic and microbiological properties, sources, and ways they interact with

* Corresponding author. Finnish Meteorological Institute, Helsinki, Finland.
E-mail address: mikhail.sofiev@fmi.fi (M. Sofiev).

https://doi.org/10.1016/j.envres.2022.113798
Received 30 March 2022; Received in revised form 7 June 2022; Accepted 27 June 2022
Available online 7 July 2022

environment (Delort and Amato, 2017; Fröhlich-Nowoisky, 2016). Interest to bioaerosols originates from several directions, such as biodiversity monitoring, environmental epidemiology and, in particular, allergology, agriculture, climate forcing, and climate change impact (Buters et al., 2018; Cecchi et al., 2010; D'Amato et al., 2007; Guxens et al., 2016; Sofiev and Bergmann, 2013; Ziska et al., 2011, 2019).

Bioaerosols are produced by biological sources and include bacteria, fungal spores, viruses, pollen, algae, etc. (Després et al., 2012). These biological particles can act as ice nucleating particles and cloud condensation nuclei in the atmosphere, thus interplaying with climate change at regional and global scales (Creamean et al., 2013; Kanji et al., 2017; Morris et al., 2014). Exposure to these particles can adversely affect human health, plants, livestock, and ecosystems (Fröhlich-Nowoisky, 2016; Hervàs et al., 2009; Humbal et al., 2018; Jorquera et al., 2015).

Culture-based and optical microscopy are the most commonly used techniques in studies of spatiotemporal distribution of bioaerosols (Banchi et al., 2018; Kraaijeveld et al., 2015; Schäfer et al., 2017; Yuan et al., 2017). However, there are several drawbacks of these conventional methods. Culturing methods are incapable of identifying many of the environmental bioaerosols because they are not viable or cultivable (Després et al., 2012; Marcovecchio and Perrino, 2021). The microscopic identification suffers from limited number of samples, which can be analysed, and insufficient distinctive morphology; these methods are also known to be time and labour-intense (Núñez et al., 2016; Sauvageat et al., 2020). The temporal resolution is another limitation, which makes it difficult to follow the dynamics of the processes (Tang et al., 2021).

Molecular-level identification shows very wide biodiversity in various environmental media (Banchi et al., 2020; Ji et al., 2013; Thomsen and Willerslev, 2015; Valentini et al., 2016). The polymerase chain reaction (PCR) is one of the most used methods enhancing detection of specific types of biotas in samples, recently applied also to identification of airborne grass pollen (Brennan et al., 2019). It amplifies DNA markers of interest, being highly sensitive and capable of detecting even a single fungal spore in a sample (Yamamoto et al., 2011). Other methods targeting specific molecules, such as a recombination factor C procedure, were recently applied to identify bacterial infection of Artemisia pollen (Oteros et al., 2019). There have been several studies investigating plant biodiversity using the DNA barcoding of pollen grains (Hajibabaei et al., 2007; Joly et al., 2014; Kress et al., 2005). The DNA barcoding approaches, however, had limited utility in mixtures of multiple species (Bell et al., 2019; Garlapati et al., 2019). Recent advances in environmental DNA (eDNA) metabarcoding and High-throughput sequencing (HTS) have provided the means to solve the issue of mixed-species identification (Kraaijeveld et al., 2015; Rojo et al., 2019; Sickel et al., 2015).

Apart from high labour costs of manual methods, regular monitoring of bioaerosols in the air has been sparse also due to a lack of automated monitoring technologies (Buters et al., 2018; Clot et al., 2020). In absence of affordable general-purpose tools, attention has been given to specific types of bioaerosols, for which comparatively easy solutions were found. The most-studied type of bioaerosols is pollen, for which the multi-decade time series are available in several parts of the world (Cecchi et al., 2010; D'Amato et al., 2007; Sofiev and Bergmann, 2013; Ziska et al., 2019). Its regular observations started almost a century ago, whereas the device used till today was suggested in late 1940s (Hirst, 1952).

A recent breakthrough in pollen (and, eventually, fungal spores) monitoring technology was brought about by two techniques: image recognition and air-flow cytometry, or a combination of both (Huffman et al., 2019). Their particle type identification algorithms rely on machine learning techniques of varying levels of complexity (Crouzy et al., 2016; Oteros et al., 2015; Šaulienė et al., 2019; Sauvageat et al., 2020). Development and evaluation of these techniques showed their high potential but also highlighted numerous challenges to overcome (Tummon et al., 2021).

The experimental campaign introduced in this paper aimed at evaluation and intercomparison of several bioaerosol monitoring approaches and had two main goals:

(i) to follow/explore the biological composition of atmospheric aerosols through the transition period from winter to summer in Northern Europe with high temporal resolution
(ii) to estimate the feasibility of bioaerosol monitoring performed on a regular operational basis and find the most-efficient approaches and observation protocols suitable for this task.

The aim of the current paper is to introduce the campaign, its approaches, and show an example of the data obtained during the first day of observations. Due to a vast amount of data generated during the campaign, detailed analysis of the results is left to follow-up publications.

2. Methodology

2.1. Setup of the campaign

The bioaerosol campaign was performed at two locations in parallel. In Helsinki, it was organized at the Station for Measuring Ecosystem - Atmosphere Relationships (SMEAR-III) and on the roof of the Finnish Meteorological Institute (FMI) main building (N 60° 12′ 15″ E 24° 57' 39", 18 m above ground level).

The SMEAR-III and FMI's main building are located next to each other on top of a wide hill 26 m above sea level. The place is an urban background area ~3 km from the city centre and 4 km from the coast of the Gulf of Finland (the nearest small bay is within 1 km). The surrounding area is rocky and consists of low vegetation, patched forest of birch (*Betula)*, aspen (*Populus*), buildings, parking lots, and small streets. A more thorough description of the SMEAR-III station and its surrounding area is given by Vesala et al. (2008). The standard pollen time series were collected at the roof of the biological department of University of Helsinki in Viikki suburb (the site FIHEVI of European Aeroallergen Network https://www.ean-net.org/, visited March 26, 2022), about 3 km from the SMEAR-III site and the FMI building.

In Siauliai, a city located about 100 km south of the Gulf of Riga, the sampling was performed on the roof of the building belonging to Šiauliai Academy of Vilnius university (N 55° 55′ 36″, E 23° 18′ 32", 128 m above sea level, about 18 m from the ground). It is located in downtown of Šiauliai near a large railway junction. Greenery covers about 19% of the surrounding territory. Lime (*Tilia*) constitutes 54% of all trees, *Betula* covers about 4%, similar to maple (*Acer*) and thuja (*Thuja*).

Collection of airborne bioaerosol samples was performed daily in Helsinki and Šiauliai during the local springtime: 3 March – 7 May in Šiauliai and 12 March – 31 May in Helsinki. Temporal resolution of the sampling was 2 h in Helsinki (6 h during the first week of the campaign) and 2.4 h in Šiauliai (10 samples per day).

The campaign combined several observation technologies in a complementary manner, but also maintained significant redundancy between new technologies and more classical approaches. This redundancy was used for evaluation of quality and reliability of the new methodologies and their cross-verification.

2.2. Aerosol monitors

2.2.1. Flow cytometer

Automated online pollen monitoring was performed with Poleno Jupiter airflow cytometer (Swisens AG, Switzerland). The device reconstructs the particle shape from its holographic image, measures particle UV-induced fluorescence, as well as optical polarization characteristics and light scattering. The effective flow rate for this device is 40 l min^{-1}, which allows the device to operate at coarse-particle concentrations up to 30 000 particles m^{-3} without overloading the

computing unit. For higher concentrations, every n-th particle is analysed, with n depending on the actual unit load.

2.2.2. Filter collector

An aerosol filter sampler (Micro-PNS-S7, MCZ Umwelttechnik GmbH) was installed on the roof of the Finnish Meteorological Institute. This method is a reference for gravimetric particulate mass measurements (EVS-EN 12341:2014) when used for PM_{10} or $PM_{2.5}$ observations. The filter collector utilizes an internal pump regulated by a mass flow controller. The flow rate, calibrated prior to the campaign, was adjustable up to 50 l min^{-1}. In the actual setup, depending on conditions, the sustainable rate provided by the pump varied between 20 and 25 l min^{-1}, controlled by the ambient temperature and pressure sensors of the sampler. The actual flow rate during each sampling interval was used in the analysis. The sampler collected particulate matter on an individual 47 mm filter (Whatman® Isopore 0.2 μm PC Membrane) located at the tip of the sample tubing. For the campaign, total suspended particles (TSP) coarser than ~0.1 μm were collected with a 24-h sampling period.

2.2.3. Standard pollen monitoring with hirst-type trap

Standard pollen monitoring was performed with Burkard 7-day pollen traps (Burkard Manufacturing Co Ltd., UK) based on the Hirst design (Hirst, 1952) in both Helsinki and Siauliai. In Siauliai, the trap was located next to the filter collector, whereas Helsinki had two sample points. The main routine observations were conducted at the roof of the biological department of University of Helsinki in Viikki suburb about 3 km from the FMI building. During the last three weeks of the campaign, a Lanzoni 2000 trap (also Hirst-type, Lanzoni S. r.l., Italy) was additionally installed at the FMI roof for a more direct comparison with the other devices.

The traps operate at 10 l min^{-1} of air flow set with the standard Burkard flow meter, which, according to (Oteros et al., 2017), is likely to lead to an effective collection rate of at least 11–12 l min^{-1}. The device locations and counting protocols followed the EAS-EAN requirements (European Aerobiological Society – European Aeroallergen Network (Galán et al., 2014; Jäger et al., 1995)).

2.2.4. Collection of samples for eDNA on sticky slides

Time-resolving sampling for DNA analysis was organized both in Helsinki and in Siauliai via collection of coarse particles onto sticky slides. In Helsinki, it was a Burkard trap with one-day clock cycle. The tape was replaced daily and cut to 12 equal-length pieces thus providing 12 bi-hourly samples per day. In Siauliai, the Rapid-E particle counter (Plair SA, Switzerland) was used for the slide collection. Its revolving mechanism automatically collected samples on 10 individual glass slides (diameter 20 mm) during the day. The principle of the aerosol collection on the slides is the same as that of the Hirst-type sampler. However, the flow rate was 2 l min^{-1}, with the corresponding changes in the collection geometry securing the capture of particles with aerodynamic diameter exceeding ~10 μm. The slide set was changed manually once per day. Sampling covered the period from the 3rd of March until the 7th of May in 2021. Utilization of the Rapid-E real-time flow cytometry capabilities was not possible due to a technical problem with the device.

2.2.5. Biospot impinger

The BioSpot™ 300 bioaerosol sampler (Aerosol Devices Inc., Colorado, USA) uses laminar-flow water condensation technology for gentle collection of biological particles sized 5 nm to >10 μm into liquid or on dry collection plate by impingement. The aerosols enter BioSpot through a single inlet and are then directed into eight three-staged growth tubes. A supersaturated water vapour environment is maintained in the growth tubes and the three stages of adjustable temperatures allow flexible management of vapour profile. Each tube has three nozzles at its end. The flow rate in each tube is 1 l min^{-1}, so the total flow rate in the device is 8 l min^{-1}. The samples were collected into 1 ml of autoclaved ion exchange cartridge purified water (MQ) with 0.1 M EDTA for DNA preservation.

2.2.6. Nanopore 3rd generation DNA sequencer

The third-generation sequencing (also referred to as the long-read sequencing) has been developed recently aiming at a portable high-throughput technology with increased read length compared to the so-called next-generation sequencing (in-essence, the second-generation technology). There are currently two main companies with commercially available devices: Pacific Biosciences (PacBio, Pacific Biosciences of California Inc., USA) and Oxford Nanopore Technologies (ONT, Oxford Nanopore Technologies plc, UK).

Nanopore sequencers are based on innovative technology of nano-scaled holes, nanopores. The nanopores are nested in a solid-state membrane of electronics and are submerged in an electrolyte solution. A voltage is applied through the membrane creating electric field that drives charged particles, e.g., DNA molecules, through the pores. As the DNA molecule strand passes through the pore, each base has a characteristic effect on the current that passes through the nanopore thus enabling base recognition of the nucleic acid sequence of the passing DNA strand. Due to nanopore sensitivity to charged particles, the purity of the sample is important for successful sequencing.

The porous membrane is located on the flow cells that are inserted into sequencing device. For this campaign, a Nanopore GridION benchtop device was selected for its compactness, high throughout and integrated computing power. The device can perform sequencing with 5 flow cells simultaneously, which, combined with the multiplexing technique, allows for up to 60 samples processed in parallel. A typical sequencing time is 6–12 h.

2.3. Modelling support of the campaign: SILAM atmospheric composition model

The System for Integrated modeLling of Atmospheric coMposition (SILAM, http://silam.fmi.fi) is an offline global-to-meso-scale chemistry transport model developed for evaluating atmospheric composition and air quality (Sofiev et al., 2015b), emergency decision support applications (Sofiev et al., 2006), source inversion problems (Sofiev, 2019; Vira and Sofiev, 2012), and analysis of observations (Meinander et al., 2020; Tarasova et al., 2007). The transformation modules cover chemical and physical reactions in the troposphere and the stratosphere (Carslaw et al., 1995; Damski et al., 2007; Gery et al., 1989; Kouznetsov and Sofiev, 2012; Sofiev, 2002, 2000; Sofiev et al., 2010).

The model is driven by meteorological and anthropogenic emission data. Biogenic emissions include pollen, aphids, and volatile organic compounds, all computed online. Other online modules for natural emission include sea salt, wind-blown dust, fire smoke, and oceanic dimethyl sulfide emissions (Korhonen et al., 2008; Poupkou et al., 2010; Soares et al., 2015; Sofiev et al., 2011, 2012).

SILAM has been evaluated in a variety of regional and global studies (Brasseur et al., 2019; Huijnen et al., 2010; Kouznetsov et al., 2020; Petersen et al., 2019; Sofiev et al., 2020, 2015a; Xian et al., 2019).

SILAM was used for two tasks: (i) modelling the concentrations of several pollen species and air quality parameters, (ii) computation of the observation footprints. The footprints were calculated for three types of species: inert weightless non-depositing tracer, fine particles 0.5 μm of dry diameter, and coarse particles with 18 μm of dry diameter. Such set of footprints corresponded to the sampling/monitoring capacities of the devices: Hirst and Rapid-E sampled particles coarser than ~5 μm, Poleno – starting from ~4 μm, whereas the filter collector and Biospot were able to capture also sub-micron aerosols.

2.4. Monitoring and sampling protocol

Detailed sampling and analysis protocols are presented in Annexes 1 and 2, respectively. Here, we present their outlook.

In Siauliai, the samples collected with the Rapid-E sampling mechanism were pre-processed in the laboratory in clean conditions, where the biogenic material from the slide was washed out to a buffer, cooled to −80 °C and stored for subsequent transfer to Helsinki in a cold pack. Each washed slide was checked under microscope to ensure that all particles were removed.

In Helsinki, real-time monitoring, sampling, processing, and DNA sequencing were distributed between the SMEAR-III station, FMI, and University of Helsinki laboratories (Fig. 1, Table 1).

Real-time monitoring was performed with Poleno Jupiter at the FMI roof. The data were processed to aerosol concentrations and presented in two different forms: as hourly-mean aerosol size spectrum for particles coarser than 4 μm of diameter, and as hourly concentrations of 10 recognized pollen species (plus mist droplets). The time series were opened to public access at https://en.ilmatieteenlaitos.fi/atmospheric-bioaerosols-modelling (visited May 26, 2022).

The core of the daily sampling for DNA analysis in Helsinki was a Burkard trap with a special clock making a full drum revolution within 24 h. The tape was subsequently cut to 12 pieces. All manipulations were performed in clean conditions.

A parallel daily sampling on filter was organized with the higher sampling volume (~20 l min^{-1}) and stricter flow monitoring than that of Burkard, which resulted in larger aerosol amounts on the filter and accurate information on the sampled air volume.

Experimental sampling directly into water was attempted with the Biospot to verify the procedure and to estimate advantages and drawbacks of this approach. The sampler does not have an outdoor encasement and was therefore set in a SMEAR-III container at the ground, with the inlet located at ~5 m above the ground. Regular collection throughout 24 h turned out to be impossible due to water evaporation or over-filling of the receiving Petry dish. In the end, the Biospot sampling was confined to daytime with frequent manual inspection of the water level and the inflow. Data of acceptable quality were obtained for the last two weeks of the campaign.

Table 1
Elements of the campaign, locations, and installed devices with their primary roles. More detailed descriptions of the devices are in the following sub-sections.

Sample collection	
Finnish Meteorological Institute (FMI), Helsinki, roof	
Poleno	Real-time flow cytometer, size-resolved particle counter, species recognition
Filter collector	Total-PM collection on filter
Burkard-24 h	Pollen and spore trap of the Hirst design with modified 24-hrs-revolution clock; sampling on sticky slides for DNA sequencing
Lanzoni	Classical pollen and spore trap of the Hirst design, particle collection on sticky tape for microscopic analysis
SMEAR-III station, Helsinki, next to the FMI main building	
Biospot	Impinger: particle collector into a liquid buffer
University of Helsinki (UHEL) biological department, Viikki, roof	
Burkard-1wk	Classical pollen and spore trap of the Hirst design, particle collection on sticky tape for microscopic analysis
Vilnius University, Siauliai Academy (SA), Siauliai, roof	
Rapid-E	The cytometer was used for automatic collection of particles on sticky slides for further eDNA analysis in Helsinki
Burkard	Classical pollen and spore trap of the Hirst design, particle collection on sticky tape for microscopic analysis
Sample analysis in laboratories and computing	
FMI laboratory	Samples preparation and pre-processing, device maintenance
University of Helsinki lab	Samples main processing: cleaning, DNA extraction, purification, sequencing with 3rd-generation techniques
SA lab	Preparation and pre-processing of Rapid-E sticky slides for transfer to UHEL laboratory; microscopic analysis of Burkard tape
University of Turku lab	Microscopic analysis of Lanzoni and Burkard tapes
FMI computing centre	SILAM model computations, bioinformatics

2.5. Analytic protocol

2.5.1. Analysis of poleno flow cytometer time series

The particle recognition algorithm employed in this campaign for Poleno measurements is based on the convolutional neural network proposed by Sauvageat et al. (2020). It utilizes supervised-learning techniques to train the neural network to classify the particle in accordance with pre-recorded calibration datasets, which consisted of species common for Southern Finland.

The recognition algorithm uses the open-source software library Keras with TensorFlow as an environment for machine learning.

2.5.2. DNA extraction and sequencing

The samples collected by the devices were supplied to a multistep DNA extraction process in order to extract all available sequencing material in high purity (see detailed protocol in Annex 2). Briefly, the extraction process started from a degradation of cell walls and

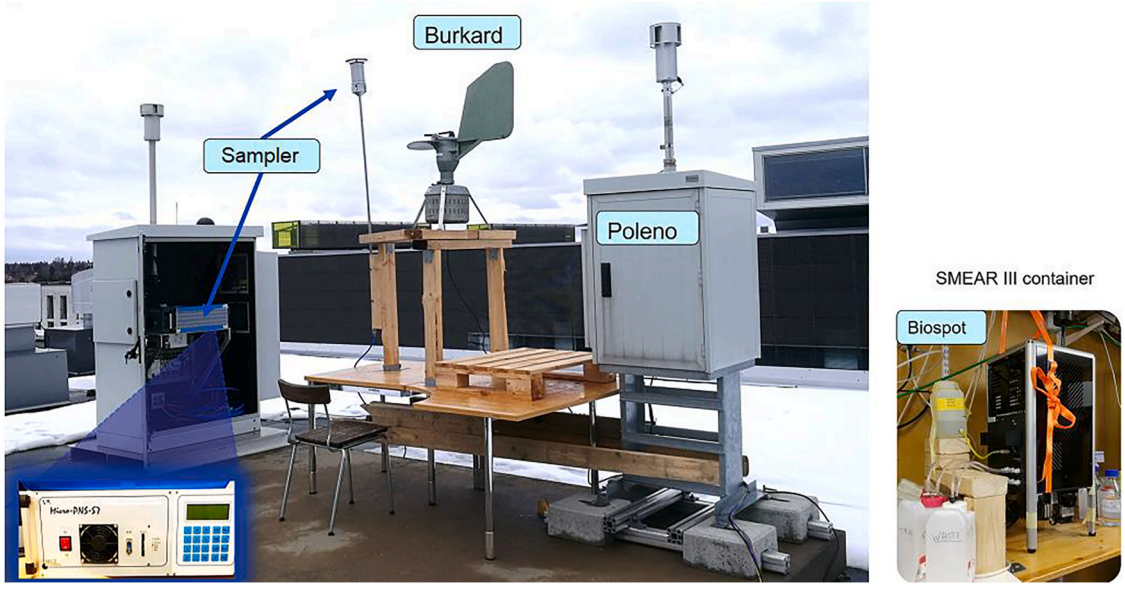

Fig. 1. Setup of the aerosol monitors at the roof of FMI and Biospot in the SMEAR-III container at 50 m.

membranes using enzymes and detergents (Harrison, 1991; Shehadul Islam et al., 2017; Woldringh, 1970), after which the cell debris and proteins were precipitated using phenol-chloroform-isoamyl alcohol method (Sevag et al., 1938). The DNA was precipitated from the aqueous phase with sodium acetate and isopropanol and the collected DNA was washed with ethanol (Li et al., 2020). The yield and purity were measured using Nanodrop 2000 spectrophotometer. Based on the obtained yield, one of two options for library preparation and sequencing was chosen: Rapid Barcoding or Rapid PCR Barcoding sequencing. Out of library preparation kits provided by ONT, the Rapid-kits with multiplexing were selected to enable the full analysis of all samples provided by the campaign. The Rapid-technology requires minimal time for the library preparation and has a multiplexing option, which allows sequencing 12 samples in each flow cell. The protocols for the kits were provided by ONT and have been used with a few modifications presented in the detailed protocols in Annex 2.

The produced sequence data were demultiplexed and trimmed from both ends using quality threshold Q7 with Cutadapt version 2.7 (Martin, 2011). Parameters of the trimmed reads were specified with Geneious Prime version 2020.2.2 (Table 2) and the reads from samples of the same device were pooled together to form daily read samples for each device. Reads were de novo assembled into contigs in Geneious assembler with medium sensitivity. The taxonomy of the assembled sequences was determined using Kraken version 2.0.8, which proved to be efficient in terms of time consumption and accuracy of assigning taxonomic labels to simulated metagenomic test sequences (Wood et al., 2019; Wood and Salzberg, 2014), and visualized with Pavian (Breitwieser and Salzberg, 2020). Species identification was performed against a custom library PlusPFP constructed for public use by Langmead et al. containing referenced sequences from NCBI database (RefSeq) for plants, fungi, bacteria, archaea, protozoa, viruses, plasmids, human genome and UniVec (NCBI-supplied database of vector, adapter, linker, and primer sequences) (https://benlangmead.github.io/aws-indexes/k2, accessed February 17, 2022). The reads that were identified to be related to human genome were removed upon detection and were not uploaded into the sequence database.

2.5.3. Delineating the origin of the observed aerosols and modelling the pollen season

The origin of the observed species and ways the atmospheric transport affected each collected sample were calculated by the SILAM model via footprint computations based on the adjoint formalism (Marchuk, 1995; Meinander et al., 2020; Tarasova et al., 2007; Veriankaitė et al., 2010). The computations were set over Central and Northern Europe with spatial resolution of $0.1^\circ \times 0.1^\circ$ (approx. 6 km × 11 km lon-lat) and 1 h of output averaging. The footprints were computed 48 h backwards from the observation start. To reflect the wide size range of bioaerosols, footprints were computed for non-reacting aerosols, 0.5 μm and 18 μm of dry aerodynamic diameter, and for a passive non-depositing tracer.

SILAM was used for computing pollination season for 6 European plant families: *Alnus*, *Betula*, *Poaceae*, *Artemisia*, *Olea*, and *Ambrosia* (Prank et al., 2013; Sofiev, 2016; Sofiev et al., 2012, 2015a, 2017).

3. Results

Due to large amount and diversity of the campaign results, they will be analysed in a series of follow-up papers. This section contains an outlook and highlights some general features of the observed patterns.

3.1. Campaign from the bird's view: weather and aerosol time series

In 2021, spring was about two weeks late, so that the late-March conditions in Helsinki were rather resembling late winter than spring: sub-zero temperature, several tens of cm of snow cover, foggy (Fig. 2). The first week of the campaign was at the end of sub-zero temperature period, with snow and fog registered by Poleno as mist (also visible as coarse particles) and associated with low visibility registered at the SMEAR-III station. A turn to summer conditions was around 10 May when temperature raised to 15 °C.

Alnus started flowering as soon as temperature rose above zero (Fig. 3). It came in several waves at the end of March and first two weeks of April. The *Betula* flowering started in May followed by *Picea* and then *Pinus* seasons with a few interruptions due to wet weather. A confusing multitude of *Fraxinus* flowering periods is probably an artefact, as well as the appearance of *Corylus* in May and *Picea* in March (see Discussion section).

SILAM prediction (Fig. 3) was highly accurate (within 2 days) for the season start but suggested too long duration significantly over-estimating the strength of the final wave of pollination. The most-probable reason for such an unusual model behaviour was the late spring, which often leads to a faster pollen release – a mechanism presently not implemented in SILAM.

In Siauliai, the weather pattern in March was resembling that of Helsinki: middle of the month was cold (but warmer than in Helsinki, just around 0 °C), with wet snow and rain (Fig. 4). More rain came at the beginning of April and then in May, this time not correlated with Helsinki. As usual, the flowering took place 1–2 weeks earlier than in Helsinki with lower concentrations of Betula and Alnus but comparable levels of other pollen types. SILAM again predicted well the start of the season (albeit over-estimated the early long-range transport episode for

Table 2
Samples from March 12, 2021 from Helsinki and Siauliai. In RES7-samples, sampling ended on the following day. Total DNA yield extracted from the samples and the purity assessed by absorbance ratio A260/A280 was determined with NanoDrop 2000.

Sample ID	Collection time	Site	Device	DNA yield (ng)	Air volume [m3]	Extraction purity
11–12.3.2021 RES7	March 11, 2021 22:30–0:55(+1)	Siauliai	Rapid-E	1440	0.288	1.50
11–12.3.2021 RES8	March 12, 2021 0:55–3:20	Siauliai	Rapid-E	996	0.288	1.52
11–12.3.2021 RES9	March 12, 2021 3:20–5:45	Siauliai	Rapid-E	894	0.288	1.50
11–12.3.2021 RES10	March 12, 2021 5:45–8:10	Siauliai	Rapid-E	1302	0.288	1.50
12–13.3.2021 RES1	March 12, 2021 8:10–10:25	Siauliai	Rapid-E	642	0.29	1.44
12–13.3.2021 RES2	March 12, 2021 10:25–12:50	Siauliai	Rapid-E	624	0.288	1.33
12–13.3.2021 RES3	March 12, 2021 12:50–15:15	Siauliai	Rapid-E	666	0.288	1.35
12–13.3.2021 RES4	March 12, 2021 15:15–17:40	Siauliai	Rapid-E	462	0.288	1.32
12–13.3.2021 RES5	March 12, 2021 17:40–20:05	Siauliai	Rapid-E	840	0.288	1.39
12–13.3.2021 RES6	March 12, 2021 20:05–22:30	Siauliai	Rapid-E	522	0.288	1.35
12–13.3.2021 RES7	March 12, 2021 22:30–0:55(+1)	Siauliai	Rapid-E	534	0.288	1.29
March 12, 2021 BRKRD1	March 12, 2021 0:00–6:00	Helsinki	Burkard	136	2.64	1.67
March 12, 2021 BRKRD2	March 12, 2021 6:00–12:00	Helsinki	Burkard	108	2.64	1.90
March 12, 2021 BRKRD3	March 12, 2021 12:00–18:00	Helsinki	Burkard	242	2.64	1.65
March 12, 2021 BRKRD4	March 12, 2021 18:00–24:00	Helsinki	Burkard	510	2.64	1.58
March 12, 2021 Biospot	March 11, 2021 20:00–18:00	Helsinki	Biospot	98	10.56[a]	1.69

[a] Biospot air volume cannot be confirmed due to a possible overfill of the collection dish overnight and a resulting loss of a part of the sample.

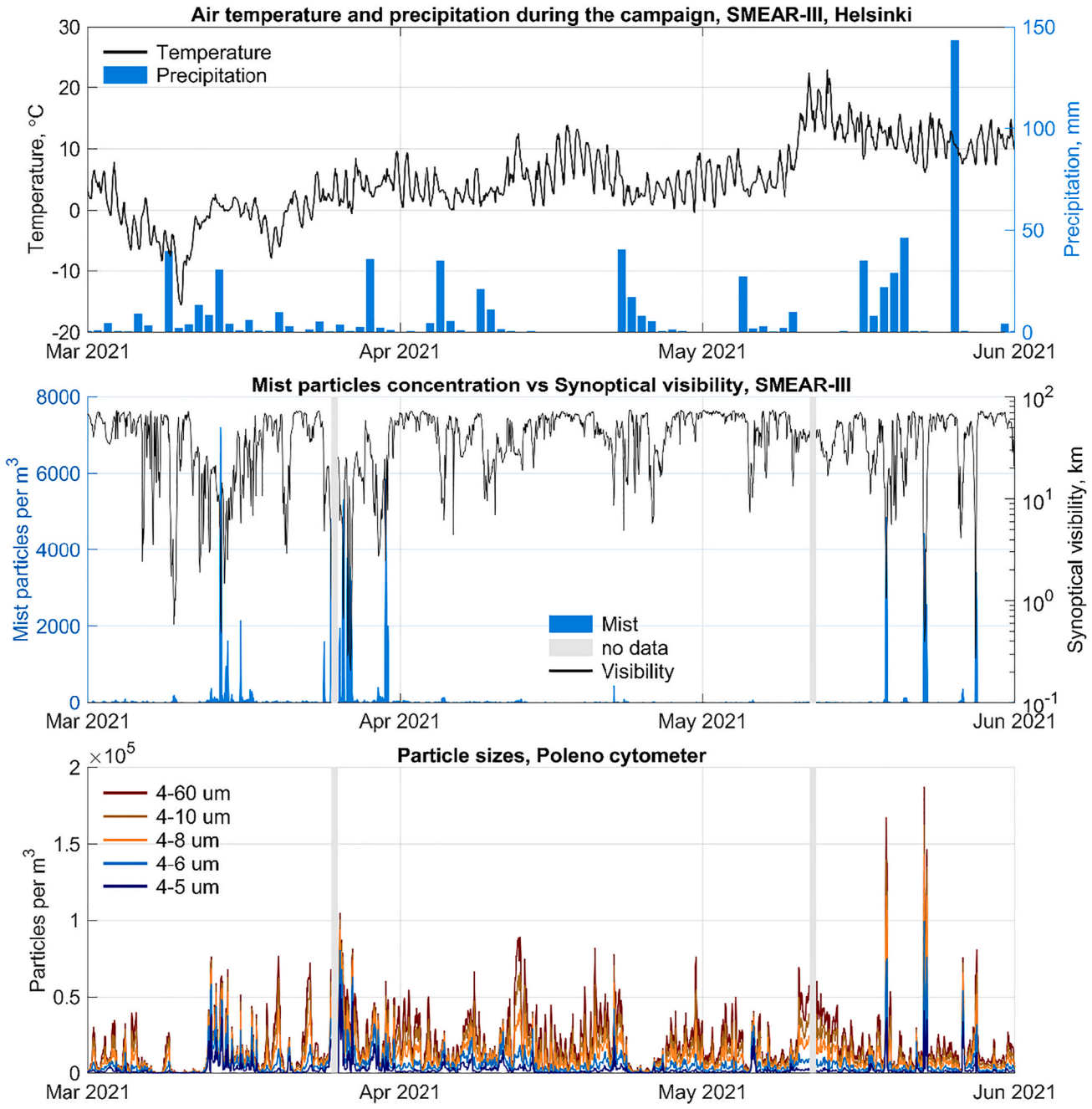

Fig. 2. Hourly time series of meteorological parameters and particle concentrations during the campaign: (top panel) air temperature and precipitation amount, (middle panel) synoptic visibility at SMEAR-III station and Poleno mist registration; (bottom panel) stacked size-segregated counts of coarse particles by Poleno. Grey shades show two days with no Poleno data. (For interpretation of the references to colour in this figure legend, the reader is referred to the Web version of this article.)

Betula) but over-estimated its duration and the strength of the late blows (Fig. 4).

3.2. Observed patterns on March 12, 2021

In this section, we present an example of the daily campaign data: observations at both locations on March 12, 2021, the first day of the campaign in Helsinki.

3.2.1. Collected samples

The first day of the Helsinki campaign with successful DNA collection on the Burkard tape was 12 March (Table 2). The clock speed was at one revolution per week, so the maximum feasible temporal resolution was 6 h. Biospot sample was collected for the period of March 11, 2021 20:00 to March 12, 2021 18:00. Daily filter sample was not collected during that day. In Siauliai, where the collection started at the beginning of March, Rapid-E slide collector provided 10 samples throughout the 24-h time period.

3.2.2. Weather conditions

The third week of March in Helsinki was particularly wet/snowy: Poleno recorded high concentrations of sub-10 μm water droplets (up to 5000 # m^{-3}) and few other particles (Fig. 2). The day of 12 March was at the start of this wet period, with the first mist case registered by Poleno.

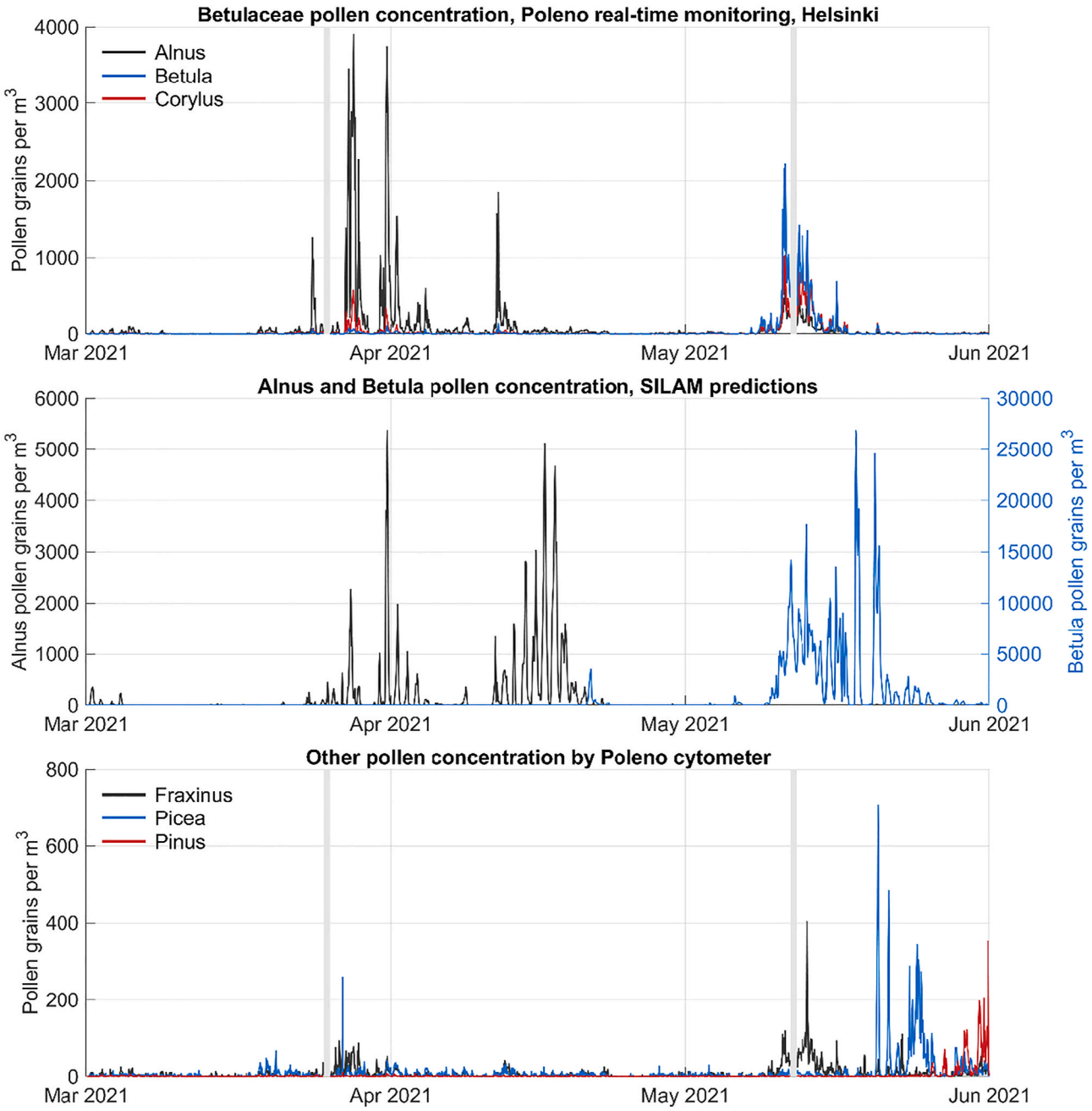

Fig. 3. Poleno observed hourly concentrations for Alnus, Betula, Corylus (upper panel), SILAM predictions for Alnus and Betula (middle panel), and Poleno observed concentrations for Fraxinus, Picea, and Pinus (lower panel). Obs. Different scales. Grey shades denote time periods with missing data. (For interpretation of the references to colour in this figure legend, the reader is referred to the Web version of this article.)

3.2.3. Sources of observed air pollutants on 12 March

The SILAM footprints computed for 12 March daytime samples at both locations (Fig. 5) show that the source areas of fine particles (0.5 μm) are to the south of the Helsinki sampling point and to the west of Siauliai. In both cases, the areas of footprint with high sensitivity were quite short (note the log-scale), owing to particle scavenging. Coarser particles sampled by Hirst and Rapid-E have even shorter range. However, the Helsinki footprint manifests, apart from a major local fraction, marine contribution from the Gulf of Finland, Tallinn regional pollution, and minor impact of Lithuania (and Siauliai). The Siauliai samples were predominantly affected by the sources at the western coast of Lithuania, with some contribution from the southern Baltic Sea. Noteworthy, some contribution in the Helsinki sample also came from the south-west along the coastal regions of Southern Baltic. That leg of the footprint overlaps with the Siauliai footprint. As a result, one can expect some (limited) similarities between the aerosol composition registered at these places.

3.2.4. Particle concentrations, DNA yield

Despite it was too early for any kind of local pollen, and coarse particles were scavenged out in Helsinki, some non-zero DNA concentrations in the air were registered at both locations (Fig. 6, obs different scales). Expectedly, Siauliai had a substantially larger concentration of bioaerosols in the air: spring had already started in Lithuania and the day was dry there. According to the footprints, majority of fine particles were from local sources in the near vicinity of the sampling points and from the area within a couple of hundreds of km from the samplers (a couple of tens of km for coarse particles).

The DNA yields obtained from the samples vary from tens of

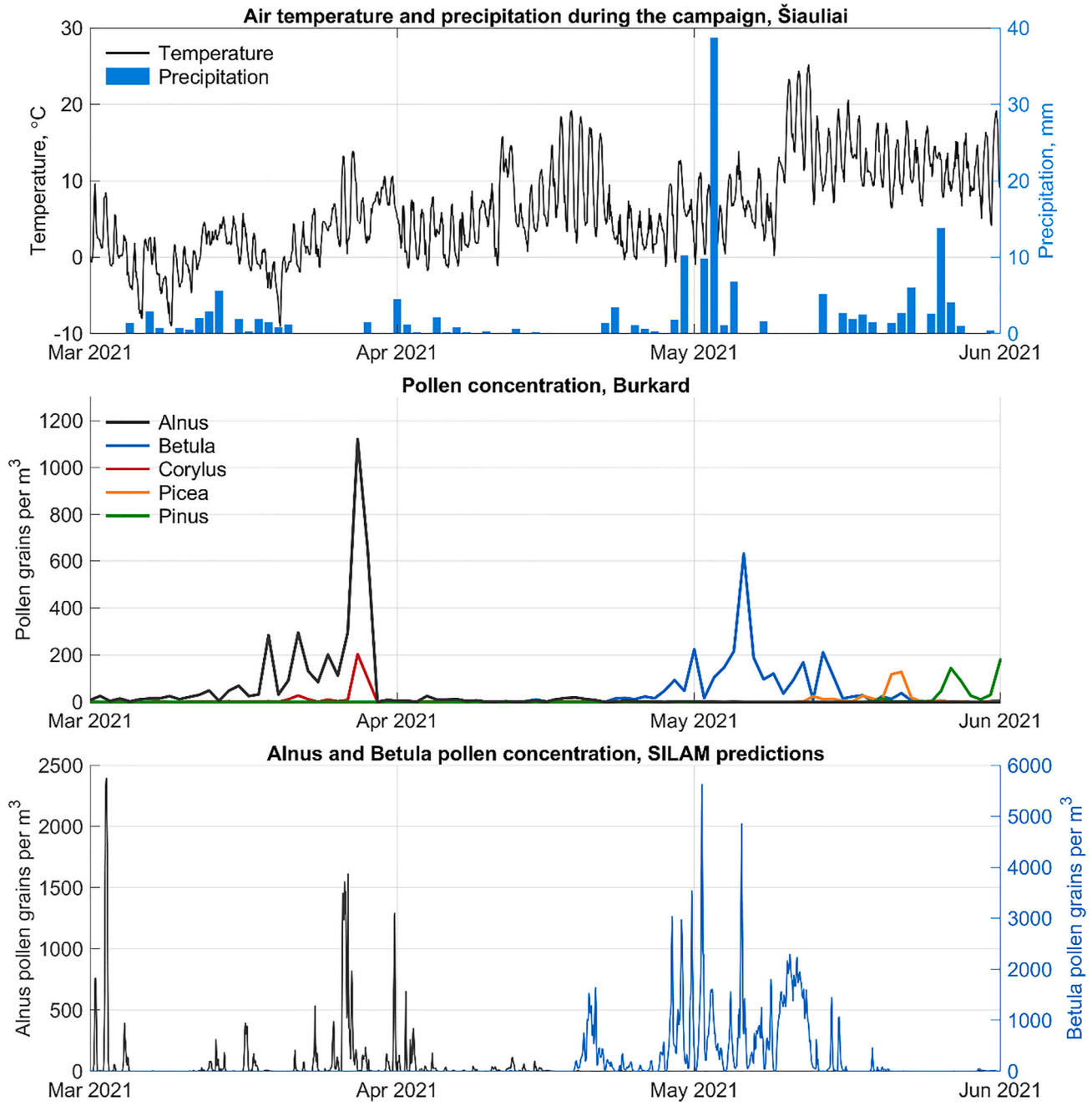

Fig. 4. Time series of meteorological parameters (top panel), observed pollen concentrations (middle panel) and SILAM predictions (lower panel) at the Siauliai sampling site.

nanograms to over a microgram of the extracted DNA (Table 2). The sample was treated with RNase A, so the RNA signal was neglected during the sample analysis. The purity of the extracted DNA assessed by absorbance ratio A260/A280 varies between 1.3 and 1.9. At the ratio of 1.8 (±0.2), a DNA sample is considered to be pure whereas the ratio below 1.6 indicates possible carryover of proteins or phenol from extraction (Gallagher, 1998; Glasel, 1995). According to this criterion, the Helsinki samples were of somewhat higher purity than the Siauliai samples. Nanopore, however, is quite tolerant to presence of small amounts of phenol in the sample, i.e., the quality of all samples was sufficient for the DNA sequencing.

An intriguing feature of the DNA yield was its independence on the "typical" diurnal cycle, which one might expect from the biologically-originated airborne particles (Fig. 6). However, in Helsinki, local flora was still frozen, which resulted in overall low concentrations (note the right-hand-side axis scale of Fig. 6), presumably dominant contribution of the remote sources in the Baltic States, and, as a result, practical independence of the DNA amount in the air from local time. Analysis of individual footprints for each observation (not shown), showed significant widening of the Helsinki footprint towards the end of the day, thus increasing the terrestrial sources contribution from the Baltic States and explaining the upward tendency of the DNA yield in Helsinki. In Siauliai (Fig. 6, left-hand axis), the changes of the transport conditions were more significant: at the beginning of the day, the air was predominantly coming from Poland with a broad footprint coverage. The pattern was rapidly evolving, so that by the morning, the western direction and narrow footprint (Fig. 5) have settled and stayed for the rest of the day. Therefore, at both sites, the DNA yield during that day rather correlated

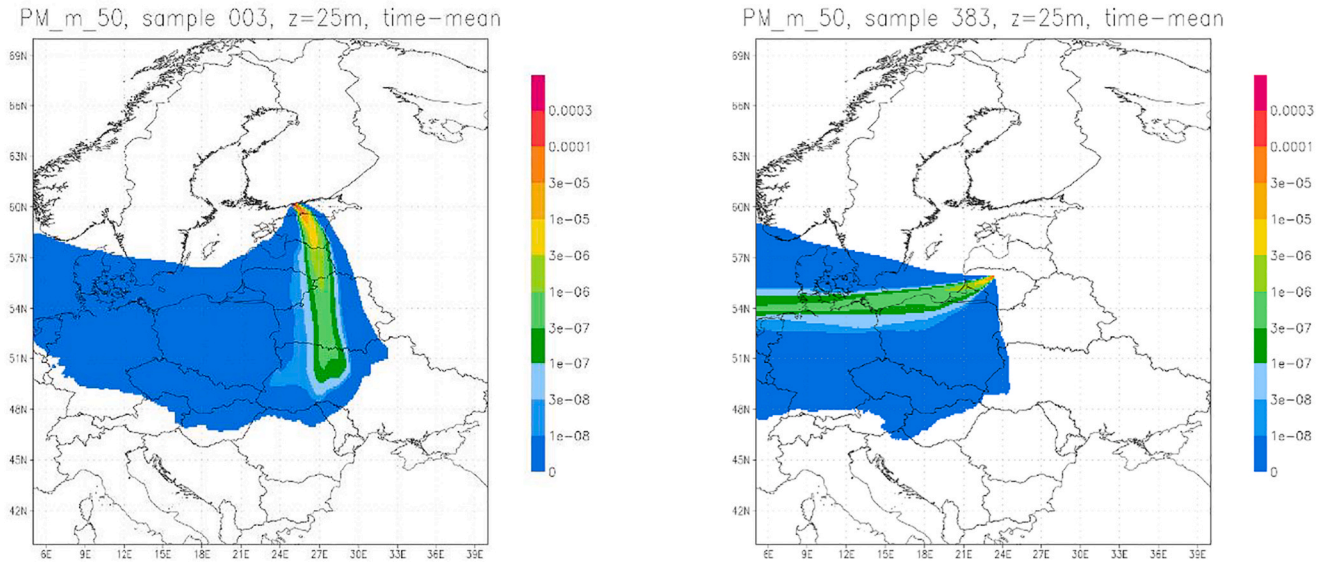

Fig. 5. Footprints for 0.5 μm particles for Helsinki (left) and Siauliai (right) for the mid-day samples on 15 March. Relative units. Obs log-scale indicating quite small area of high sensitivity of the sample to the particle sources.

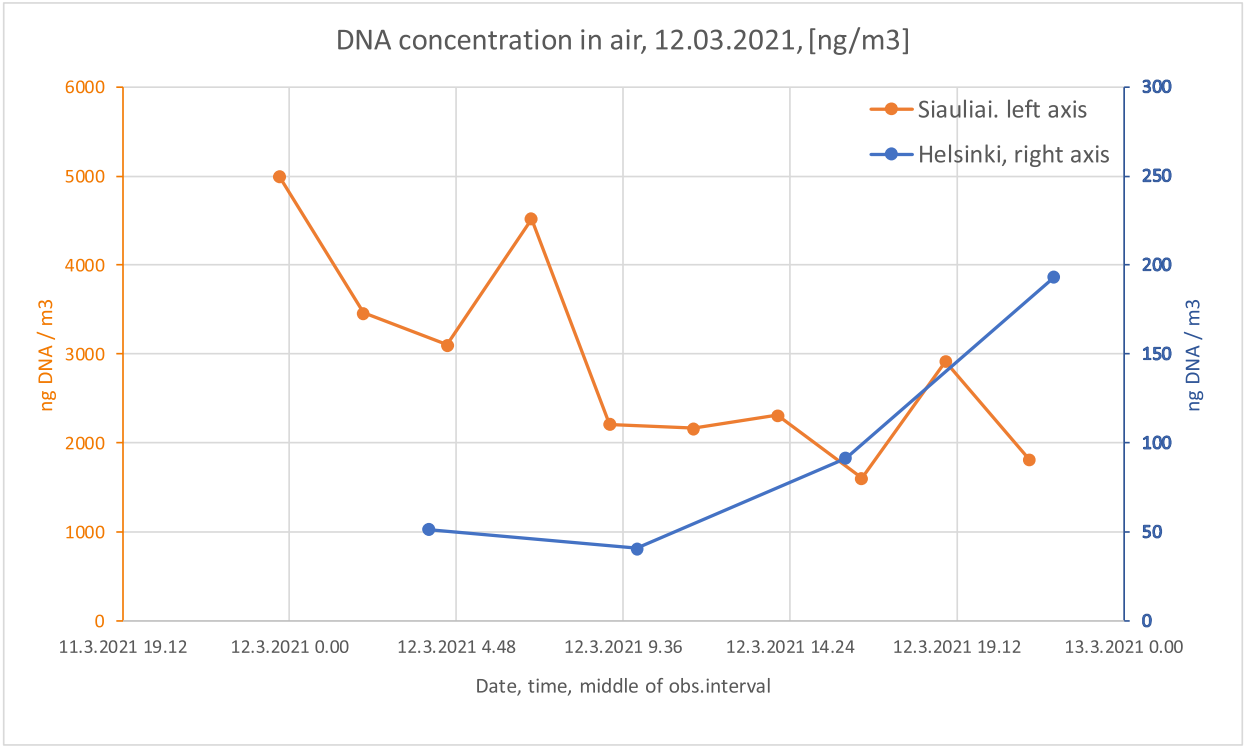

Fig. 6. DNA concentration in the air, March 12, 2021, [ng m^{-3}]. Note 6-hourly resolution in Helsinki and 2.4 h in Siauliai. Dots denote the middle of the corresponding sample periods. Obs different scales.

Table 3
Sequence data parameters prior to processing. Accession numbers were acquired upon submission of raw read sequence to the ENA database https://www.ebi.ac.uk/ena/browser/home, (access June 2, 2022) project number PRJEB50978.

Accession number	Sequencing sample ID	Total sequence length (Kb)	% GC	Min. read length (nt)	Max. read length (nt)	Assembled contigs	N50	Unused reads
ERS10608455	Rapid-E March 12, 2021	2899	44	150	2726	1236	449	2666
ERS10608454	Burkard March 12, 2021	500	42	150	10 215	347	351	1678
ERS10608453	Biospot March 12, 2021	83.6	39	150	16 630	54	330	232

with the transport conditions and contributions from remote regions rather than with the diurnal activity cycle of local sources.

3.2.5. Biological composition of the collected samples, March 12, 2021

Metagenomic sequencing produced varying total length and the number of reads with highly diverse read lengths. After demultiplexing and trimming the low-quality ends from the reads (Table 3), contigs were assembled with N50 length varying from 330 to 449 bp and GC-fraction ranging from 39% to 44%.

Contigs and reads not used in the assembly were identified with Kraken and visualized as Sankey diagrams with Pavian (Fig. 7 A-C (Breitwieser and Salzberg, 2020),). The results show that majority of the classification hits are in the bacterial domain. Out of all contigs and reads unused in the assembly, 45%–58% were successfully classified with Kraken, which suggested that a large part, 25%–37% of the sequences, belong to unspecified chordates (Fig. 7 D).

The majority of the assigned reads from both Siauliai and Helsinki samples were identified as bacteria from Enterobacteriaceae family, mostly *Shigella flexneri*, *Escherichia coli* and *Salmonella enterica*. These species are usually implicated as infectious agents, but there was no indication of presence of pathogenic agents in the samples. Bacteria of these families also live in soil, which is the most-probable origin of those found in the samples.

Considering the fraction of reads identified as Eukaryota, in Helsinki they were all identified as the Magnoliopsida class (it was also the main Eukaryota in Siauliai, accompanied by several fungal species), detected in all samples of 12 May. The class Magnoliopsida includes a wide set of flowering plants in Europe but its presence in Helsinki air in late winter was by no means expected. The most-probable explanation for the finding is release of bioaerosols from Helsinki botanical garden located at about 1 km distance from FMI, as well as from the long-range transport. In Siauliai, spring was already on the way, so appearance of a variety of plant species in the air samples was not surprising.

One can note presence of Pseudomonadales in all samples. Many of these bacteria contribute to cloud formation acting as ice nucleation agents (de Araujo et al., 2019; Maki et al., 1974).

A significant difference between the Siauliai and Helsinki composition is the presence of a substantial fraction of actinobacteria found in Siauliai. They can partly originate from the southern Baltic Sea, but also from terrestrial ecosystems (see footprints Fig. 5). These bacteria contribute to soil ecosystems by helping to decompose the organic matter of dead organisms. Their substantial fingerprint in the Siauliai samples indicated that decomposition and growth processes have already started there, whereas the Helsinki area, Gulf of Finland and Tallinn region were still frozen and largely covered with snow.

4. Discussion

The first results of the campaign and the gained experience in maintaining the monitoring over 2 months at two locations, provided the answers to the main questions that motivated the effort:

- the first high-resolution timeseries of biological aerosols in the air of Northern Europe have been obtained

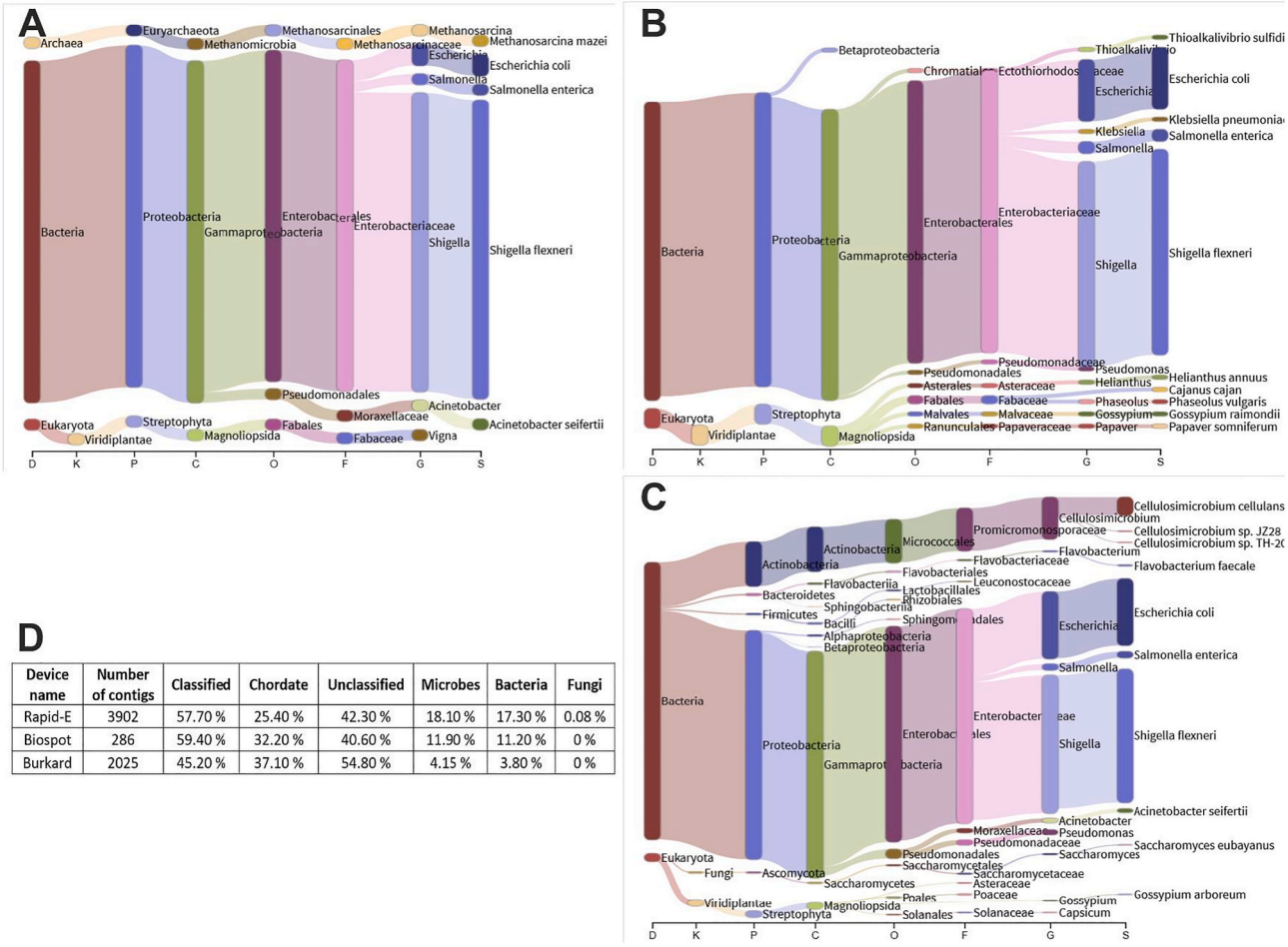

D

Device name	Number of contigs	Classified	Chordate	Unclassified	Microbes	Bacteria	Fungi
Rapid-E	3902	57.70 %	25.40 %	42.30 %	18.10 %	17.30 %	0.08 %
Biospot	286	59.40 %	32.20 %	40.60 %	11.90 %	11.20 %	0 %
Burkard	2025	45.20 %	37.10 %	54.80 %	4.15 %	3.80 %	0 %

Fig. 7. Classification of the samples, Biospot at Helsinki SMEAR-III (A), Burkard in Helsinki, FMI roof (B) and Rapid-E in Siauliai, SA roof (C), from the first day of the campaign, March 12th. Statistics of the identified contigs are shown in table D. The flow diagrams A-C illustrate the proportion of reads assigned to a specific taxon at domain (D), kingdom (K), phylum (P), class (C), order (O), family (F), genus (G) and species (S) levels.

- feasible protocols of regular monitoring of atmospheric bioaerosols have been found, strong and weak points of the devices involved in the campaign highlighted

4.1. Poleno flow cytometer: high reliability, particle identification gradually improves

Reliability of the Poleno monitor was high: 98.5% of hourly data were recorded successfully (33 out of 2207 hourly data from March 1 to May 3 were lost – note the grey bars in Figs. 2 and 3). Towards the end of the campaign, the produced data were included in the publicly accessible research Web page (https://en.ilmatieteenlaitos.fi/atmospheric-bioaerosols-modelling, accessed May 26, 2022) as the first real-time bioaerosol data in Northern Europe, and a demonstration of feasibility of operational usage of this device for bioaerosol monitoring.

As anticipated, classification of pollen and distinguishing them from other types of aerosols required fine-tuning. The identification algorithm, initially trained with dry pollen in the FMI laboratory, has been evolving throughout the campaign accounting for the real-life conditions. Thus, at the beginning, water droplets were not familiar for the algorithm, and the first fog event was used to add them to the reference datasets.

A significant *Alnus/Betula/Corylus* confusion was revealed, in agreement with our earlier studies of the Rapid-E monitor (Šaulienė et al., 2019). However, the overall accuracy, as obtained from the confusion matrix, was higher, on-par with the skills reported by other Poleno studies (Sauvageat et al., 2020). The confusion of *Betulaceae* species was asymmetric: it seems that *Alnus* and *Corylus* are correctly recognized in late February – early March with no *Betula* during that period, in agreement with climatological profiles and manual observations. But during the *Betula* pollen season, the algorithm again claims significant *Alnus* and *Corylus* concentrations, which is probably a misinterpretation: their season should be already over. Number-wise, up to half of Betula was misread as *Alnus* or *Corylus*. Certain discrepancy was also found for *Betula* absolute concentrations: even if *Alnus* + *Corylus* + *Betula* particles are combined in April, assuming all of them were *Betula*, the concentration was about-half of what was shown by the Burkard trap in Viikki (but the distance of 3 km between the monitoring locations can explain the difference).

Fraxinus seems to be confused with some other pollen in March and in June showing noticeable false positive recordings. It might be affected by some species not included in the reference datasets. For *Quercus*, the algorithm has generated a noisy signal, which was not included in the published time series.

March was a particularly difficult month because of high road dust concentrations in Helsinki. Large variability of aerosol shapes and sizes, as well as their fluorescence, challenged the recognition algorithm and resulted in a noticeable number of false recognitions.

These observations broadly corroborate with the findings of the intercomparison campaign of EUMETNET Autopollen programme that was carried out in about-same time in Munich (Tummon & Crouzy, pers. commun, Moreno et al. in prep., (Tummon et al., 2021)), as well as with the limited experience collected to-date in field applications of such devices (Huffman et al., 2019; Lieberherr et al., 2021; Sauvageat et al., 2020). In particular, difficulties with *Alnus/Betula/Corylus* separation, false positives outside the season, and some differences from the absolute values reported by the Hirst-type devices were quite common issues for flow cytometers in both campaigns. Despite these issues, both campaigns confirmed a good agreement of the Poleno time series with those of Hirst trap during the main season for most of the reported species.

With the overall good classification skills, the above issues set agenda for a follow-up device calibration combined with development of a new version of its recognition algorithm with more reliance on real-life samples and the fluorescence signal.

4.2. Regular monitoring of eDNA in the air: (some) technology can be used

With identification of biological particles by real-time monitors posing certain difficulties even for pollen, an “ultimate classifier” based on eDNA sequencing is a very tempting approach. Until recently, it was unfeasible due to high costs and labour requirements of the Next-generation sequencing devices and procedures. The development of the 3rd generation sequencing opened up this possibility (van Dijk et al., 2018). The new Nanopore technology, however, has practically not been applied to atmospheric samples. The corresponding protocols had to be developed largely from scratch. Within the campaign, they have been split to three steps: collection of particles, filter processing and DNA extraction, DNA sequencing and bioinformatics.

We have tested three techniques of collecting the biological particles from the air: (i) the standard medium-volume filter sampler, (ii) the Hirst-type pollen trap or a similar approach with a Rapid-E sampling module, and (iii) the Biospot sampler. Their performance proved to be very different rendering some of these techniques unsuitable for regular monitoring. Their overall performance during the whole campaign is illustrated in Table 4. Comparing the numbers, one should keep in mind the higher DNA concentration in the air of Siauliai than in Helsinki (Fig. 6 for March 12, 2021, sustained throughout the whole campaign). In that light, performance of Burkard was comparable to that of the filter and Rapid-E samplers, whereas Biospot essentially failed. Efficiency of Rapid-E was also quite low due to its low sampling volume (2 l min^{-1}) compared to 10 and 20 l min^{-1} for Burkard and the filter sampler, respectively. A surprising issue was that the filter sampler had collected much less DNA than Burkard despite 2x volume flow. Since the polycarbonate filter was completely dissolved during processing and the tape washed fully, the sample extraction was 100% in both cases. A plausible explanation for now is that the strong pressure drop on the filter and high air flow velocity through the pores might have damaged a fraction of the cells. The problem deserves further investigation and experimenting in controlled conditions.

4.2.1. Medium-volume total-PM sampling on filter: robust performance

The best experience in the eDNA collection has been found with the standard medium-volume total PM sampler on a hydrophilic filter. The sustainable air flow of 20–25 l min^{-1} with 24 h long sampling time provided a sufficient amount of the biological material in more than half of the cases, so that the DNA sequencing could be performed without the preceding PCR step. It greatly simplified and sped up the analytical procedure and allowed for quantitative conclusions, thus making the device suitable for regular monitoring with daily temporal resolution. However, double-to-quadruple air flow rate can be recommended to ensure sufficient biological material under all conditions. With high-throughput pumps and large-size robust filters widely used in, e.g., ambient radioactivity monitoring, it seems to be affordable. The issue of low DNA yield compared to sticky slides needs to be understood but with high-volume collection on large filters it should be not too significant.

4.2.2. Sticky slides of the hirst-type trap: works but large uncertainties and low flow rate

The primary collection technique used in the campaign was the Hirst-type trap. Its advantage compared to other samplers was the time-resolving sampling capabilities, with 6-h or 2-h resolution depending on

Table 4
Total DNA amount collected by each sampler during the whole campaign, μg.

Device	Period	DNA yield, μg
Helsinki, Burkard	12.3–31.5.2021	435.5
Helsinki, filter	16.3–31.5.2021	91.2
Helsinki, Biospot	12.3–31.5.2021	1.2
Siauliai, Rapid-E	3.3–May 15, 2021	321.0

the internal clock of the device. The visiting intervals for replacing the sticky tape were one week and one day, respectively. Transparent slides allowed explicit verification via microscope that all collected particles are washed out to the buffer. The main drawback, however, was its low flow rate (~11 l min^{-1}). As a result, even 6-hourly samples had low DNA amount (Fig. 6) and required PCR step prior to sequencing. Also, there were substantial problems with reliability, clock accuracy, and flow uncertainties, controlled and rectified during the campaign at a cost of large additional efforts and time spent for daily check-ups and maintenance. Therefore, despite its success in the campaign, this approach cannot be recommended for regular use.

4.2.3. Biospot: adaptation needed for sampling longer than an hour

The campaign showed that the maximum duration of unattended Biospot sampling cannot exceed a couple hours: the air flow either dries out the collecting liquid (if the air is too dry) or overfills the dish if the air is too moist. The device can control the air humidity by injecting water in the air flow, but the amount of added water has to be set manually and does not follow the changes in the ambient conditions. After numerous experiments, we concluded that this process can, in principle, be automated, which might make the device suitable for long unattended monitoring. However, it would require a substantial rework in the control module, which can be done only by the manufacturer. In its current version, the device is not suitable for sampling times exceeding a couple of hours.

4.2.4. Sequencing with nanopore: feasible for regular analysis

The primary challenge in sequencing the atmospheric samples was the limited amount of DNA in the sample. The PCR step, normally recommended for increasing the amount of biomaterial, proved to increase the analysis time ~10-fold, also boosting costs and hampering the quantitative estimates of the bioaerosol composition (see next section). A threshold for the DNA amount in the sample, above which the PCR step could be skipped, was empirically found to be 700 ng of DNA after its extraction. For such samples, the sequencing with Nanopore GridION of up to 60 samples per one working day proved feasible, bringing the overall costs of the whole-genome multi-species sequencing as low as 30–40 Euro per sample (all costs included). This number could be further reduced when all stages are optimized and automated wherever possible.

4.3. Obstacles in species identification and analysis of environmental metagenomes

Air is an extremely difficult environment for extracting genetic material and preserving its integrity. Since the aim of this study was to obtain metagenomics data with as complete spectrum of species in the atmosphere as possible, including microbes, fungi, and pollen, the selected DNA extraction protocol was long, multistep and complex. Obtaining sequence data from all species in the sample was prioritized to the preservation of long DNA molecules that are usually preferred in sequencing with ONT (Leggett and Clark, 2017). Introducing faster methods, such as DNA-binding silica-columns (Katevatis et al., 2017) or magnetic beads (Berensmeier, 2006) for DNA purification, would keep the metagenome of full species spectrum and shorten the DNA extraction protocol decreasing the time required for extraction thus reducing the probability of random fragmentation. This, however, might increase the analysis cost due to more expensive agents, and will require thorough compatibility testing between the sample collection and extraction protocols.

In the campaign, assignment of taxonomic labels to the reads was 40%–55% effective resulting in a large proportion of unclassified reads, which broadly agrees with previous microbiome studies from urban environments (Afshinnekoo et al., 2015; Danko et al., 2021; Hsu et al., 2016; Thompson et al., 2017), air (Yooseph et al., 2013), soil (Van Goethem et al., 2021), and water (Cao et al., 2020). Our results support the hypothesis that the air microbiome consists of previously unobserved diversity of organisms with taxa uncharacterized in the current reference sequence databases (Danko et al., 2021).

The classified reads were mainly assigned to bacteria, which was surprising given the bias of the classification due to the differences in genome sizes. Eukaryotic genomes are manifold larger than those of other domains, which was expected to create bias in classification towards the species with larger genomes. Indeed, in case of equal amount of bacterial and pollen cells in the sample, the ratio of obtained reads will significantly depend on size of the genomes. The observed prevalence towards bacteria in the samples can be potentially explained by the bias in the databases occurring due to imbalance of the reference sequences (Santamaria et al., 2012; Troudet et al., 2017) and large proportion of the unidentified sequences. Classification of reads obtained from the eukaryotic species is also obstructed due to (i) high rate of repetitive elements in their large genomes compared to other domains and (ii) a drastic underrepresentation of the reference genomic sequence data for fungi and plants not linked to human activities or needs (del Campo et al., 2014; Marks et al., 2021). A large fraction of their genomes consists of repetitive sequences, in some plants they can cover up to 90% of the genome (Mehrotra and Goyal, 2014). Therefore, a more efficient assignment of taxa can be achieved with ultra-long reads (>10 kb) to cover complete repetitive regions or broad genome- and species-specific repetitive element databases, or both (Liao et al., 2022; Wommack et al., 2008).

The incompleteness of the public genome databases challenges the BLAST (Basic Local Alignment Search Tool) search approach and requires advanced methods. Formation of specialized databases for atmospheric bioaerosols, combined with generation of the reference sets for the currently missing species is a necessary pre-requisite for high-quality bioaerosols identification via DNA sequencing.

5. Summary

The campaign has demonstrated the feasibility of regular complex bioaerosol monitoring with the combination of the automatic flow cytometer and the medium/high-volume sampling with the eDNA 3rd generation sequencing, supported by the atmospheric dispersion modelling.

The initial selection of the devices and tools for the campaign was rather opportunistic, but the working configuration was found as the first key outcome of the campaign: (i) Poleno real-time flow cytometer, (ii) the medium/high-volume daily particle filter sampling followed by the 3rd generation DNA sequencing, and (iii) SILAM atmospheric composition model, which provided footprints for each sample and forecasted air quality and pollen concentrations. Such combination of technologies has shown comprehensive results, with its components complementing each other. During the campaign, the above combination was accompanied with the classic Burkard traps serving as a link to the familiar technology.

Apart from the technological tasks, the campaign also provided the first high-resolution dataset on the bioaerosol composition in the Northern-European spring season.

The identified plant species belong to Magnoliopsida, which were detected in practically all samples. The class Magnoliopsida includes a wide set of flowering plants in Europe. A small fraction of fungal species was noticed in Siauliai. A more specific identification is pending upon construction of specialized DNA databases oriented to atmospheric biota: the generic DNA databases do not contain the needed species.

Much more detailed information was available for bacteria, albeit also with a specific bias towards human health and agriculture-relevant pathogens.

Due to a lack of studies about microbiome of urban air, ~40% of the reads remained unclassified. Development of genome databases and classification methods is needed for a more accurate and complete classification of previously unobserved entities.

Data availability

Poleno monitoring data are available online at https://en.ilmatieteenlaitos.fi/atmospheric-bioaerosols-modelling. The sequence data was uploaded to the ENA database as trimmed read data and are publicly available from the project PRJEB50978, samples ERS10608455, ERS10608454 and ERS10608453. The SILAM air quality and pollen forecasts are open at the model Web site http://silam.fmi.fi.

Declaration of competing interest

The authors declare that they have no known competing financial interests or personal relationships that could have appeared to influence the work reported in this paper.

Acknowledgments

The campaign has been performed within the scope of Academy of Finland projects PS4A (Grant Nbr 318194), ALL-IMPRESS (Grant Nbr 329215), and ACCC Flagship (Grant 337552), and has been supported by the European Social Fund (project no. 09.3.3-LMT-K-712-01-0066) under grant agreement with the Research Council of Lithuania (LMTLT). Discussions with Letty De Weger (Medical University of Leiden) and support of Jeroen Buters (Technical University of Munich) are greatly appreciated. We also would like to thank two anonymous reviewers, whose detailed comments helped us to improve the paper.

10. Annex 1. Detailed sampling protocol

Rapid-E, Siauliai. The slide changing mechanism of the Rapid-E counter was used for the slide collection in Siauliai, on the roof the building belonging to Šiauliai Academy of Vilnius university (N 55° 55′ 36″, E 23° 18′ 32″). The building height is about 18 m from the ground and 128 m above sea level. The revolving mechanism automatically collected samples on 10 individual glass slides (diameter 20 mm) during the day. The principle of the aerosol collection on the slides is the same as that of the Hirst-type sampler. However, the flow rate was 2 l min^{-1}, with the corresponding changes in the collection geometry securing the capture of particles with aerodynamic diameter exceeding ~10 μm. The slide set was changed manually once per day. Upon collection, the slides were moved to VU laboratory, and the collected material from each slide was washed into 1 ml of Longmire's buffer by incubating for 5 min. After gentle shaking, the liquid was moved to an Eppendorf tube. The washed slide was checked under the microscope for pollen to ensure that all the particles were removed. Extracted DNA samples were stored at −80 °C until transported to Helsinki in a cold pack.

BIOSPOT, Helsinki. The device was approached three times each day. During the first visit, the working parameters were checked, after which the device was stopped to pick up the Petri dish with the collected sample. After that, the Petri dish was covered with lid and sealed with parafilm, then placed in the cold box to deliver to the lab. The Biospot supplementary bottles were emptied, and 70% ethanol was filled to the input Supply bottle for the device cleaning round (1000 injections) while the air inlet was protected with a particle filter. The cold box was delivered to the lab where the liquid sample was moved from the Petri dish into the Eppendorf tube and placed in the lab freezer (−20 °C). The second visit to the Biospot upon completion of the ethanol cleaning started the additional cleaning step with Milli-Q Water (also 1000 injections). Finally, the third visit was used to set the new Petri dish filled with 1 ml of Buffer A (0.1 M EDTA, pH 7.5), refill the input Supply bottle with Milli-Q Water and program the new measurement period (6 h during daytime of the next day).

Sampler on filter, Helsinki. The 24-h sample was collected on the hydrophilic filter (Whatman® Isopore 0.2 μm PC Membrane filter). Upon exposure, the filter was moved to the FMI lab and the collected material was washed into Eppendorf tube with 1 ml of Buffer B (Longmire's buffer without SDS: 0.1 M Tris-HCl, 0.1 M EDTA, 0.01 M NaCl, pH7.5) and placed to the lab freezer (−20 °C).

Hirst-type traps, Helsinki. During the first two weeks of the campaign, the Burkard trap was operated with the standard 7-days clock, which was subsequently switched to 24 h clock to increase temporal resolution. The drum was covered with Melinex tape and coated with adhesive grease (toluene and Vaseline mixture). The drum, the tape, and the transport canisters were cleaned with 70% ethanol every time before the usage. Adhesive liquid was spread over the tape with sterile (single use) swab. Upon exposure, the tape was cut to 28 (first two weeks, 6 h of exposure per sample) and 12 pieces (rest of the campaign, 2 h exposure per sample). Each tape fragment was placed into the Eppendorf tube (marked and pre-filled with 1 ml of Buffer B), shaken and moved to the lab freezer (−20 °C).

All processing steps were performed in clean conditions, with face masks and hair covers, lab coats, and gloves. The instruments were either single-use or sterilized with ethanol before processing the next sample. The inlets of Poleno, Biospot, and Filter collector were regularly cleaned throughout the campaign with ethanol while the Burkard orifice was cleaned from debris with compressed air every time at the tape replacement. The daily routine for 4 devices was taking about 2.5 h. Every 2–3 days, the frozen samples were moved from the FMI lab to the University of Helsinki lab in a cold box for the DNA extraction, analysis, and storage at −80 °C.

11. Annex 2. DNA extraction protocol

1. Add to Biospot sample 1/10 of sample volume 1 M Tris and 1/500 of volume 5 M NaCl: the buffer needs to be 0.1 M Tris, 0.1 M EDTA and 0.01 M NaCl (Buffer B, Longmire's buffer without SDS).

Cell lysis

2. Add enzymatic lysing reagents in each reaction:
   - 1 μl *of Chitinase*
   - 2 μl *of Lysostaphin*
   - 3 μl *of Lyticase*
   - 20 μl *of Lysozyme*
2. Incubate at +37 °C gently mixing at 80 rpm horizontal on shaker for 1 h.
3. Add 100 μl of 10x detergent mix per 1 ml of sample.
4. Add 5 μl of Proteinase K solution per 1 ml of sample.
   - *ex. if sample is* 2 ml*, put* 10 μl *of Proteinase K solution*

- 5 μl *for Burkard samples*
- 10 μl *for Filter collector samples*
- 10 μl for Biospot samples, sample volume varies

5. Incubate at +55 °C for 30 min in a water bath.
6. Continue to protein and cell debris precipitation.

Proteins and cell debris precipitation

7. Add volume to volume 25:24:1 phenol/chloroform/isoamyl alcohol (PCI mix).
   - *Rapid-E samples: divide into two Eppendorf tubes*
8. Vortex for 5–10 s and centrifuge for 30 min at 15 000×*g* at RT.
9. Move the upper aqueous phase of the supernatant to separate tube, discard the pellet and phenol phase.
   - *Take the volume that equals the sample volume before addition of PCI mix.*
10. If precipitated debris (white precipitate) present in supernatant, repeat steps 7–9. Aim to avoid.

DNA precipitation (all samples)

11. Add 1/10 of the sample volume of Sodium Acetate (3 M, pH 5,2) (approximately).
    - Salt neutralizes the charge on the nucleic acid backbone. This causes the DNA to become less hydrophilic and precipitate out of solution.
    - 100 μl for Rapid-E and Burkard samples
    - 100–200 μl for Biospot samples
    - 200 μl for Filter collectr samples
12. Add 0,7 of current sample volume of isopropanol.
    - Room temperature isopropanol minimizes coprecipitation of salt.
    - 700 μl for Rapid-E and Burkard samples
13. Centrifuge immediately at maximum speed for 30 min at 4 °C.
14. Discard the supernatant.
    - Be careful, isopropanol precipitated pellets are often difficult to see and loosely attached.
    - Mark outside of tube before centrifugation for easy identification.
15. Wash the pellet by adding 700 μl of 70% ethanol and pipet it gently up and down several times or gently turn the tube up and down few times.
16. Centrifuge at maximum speed for 15 min at 4 °C.
17. Discard supernatant.
18. Repeat the washing (steps 16.-18.) 3x to maximally wash out the salts.
19. Centrifuge at maximum speed for 5 min at 4 °C to get rid of residual ethanol.
20. Let the pellet air dry briefly, 5–20 min depending on the size of the pellet.
21. Gently resuspend the pellet in 20 μl of nuclease-free water of filtered MQ water.
22. Check DNA concentration as well as A260/A280 and A230/A260 ratios with Nanodrop.
23. Store at −20 °C for short term or −80 °C for long term.
24. Run 5 μl on 1% agarose gel.
25. Store at +4 °C or proceed to preparation of sequencing library.

12. Annex 3. Library preparation

Rapid Barcoding

1. In a 0.2 ml thin-walled PCR tube, mix the following:
   - template DNA 3 μl
   - Fragmentation Mix RB01-12 1 μl
   - preferred DNA yield in sample >700 ng
2. Mix gently by flicking the tube, and spin down.
3. Incubate the tube at 30 °C for 1 min and then at 80 °C for 1 min. Briefly put the tube on ice to cool it down.
4. Pool all barcoded samples.
   - *If 10–12 barcoded samples, pipet* 1 μl *of each*
   - If fewer samples, put 2 μl or more of the sample with the lowest concentration to make concentration of each barcoded sample equal to the others
5. Add 1 μl of RAP to the pooled barcoded DNA.
6. Mix gently by flicking the tube, and spin down.
7. Incubate the reaction for 5 min at RT.
8. Keep on ice until ready to load.
9. Prime the flow cell according to the Nanopore protocol.

Rapid PCR Barcoding

1. Thaw and prepare the reagents as follows:
   - Barcodes (RLB 01–12) at RT
   - Fragmentation Mix (FRM) on ice

- Rapid Adapter (RAP) on ice

2. Prepare the DNA in Nuclease-free water.
3. Transfer 1–5 ng genomic DNA into a DNA LoBind tube
   - 3 μl 1 ng/μl (1–25 ng)
   - 2 μl 1,5 ng/μl (25–45 ng)
   - 1 μl 3 ng/μl (45–90 ng)
   - 0.5 μl 6 ng/μl (90–180 ng)
   - 0.2 μl 15 ng/μl (180–450 ng)
4. Adjust the volume to 3 μl with Nuclease-free water
5. Mix thoroughly by flicking, avoiding unwanted shearing
6. Spin down briefly in a microfuge
7. In a **0.2 ml thin-walled PCR tube**, mix the following:
   - 1.5 μl 1–5 ng template DNA
   - 0.5 μl FRM
8. Mix gently by flicking the tube, and spin down.
9. In a thermal cycler, incubate the tube at 30 °C for 1 min and then at 80 °C for 1 min.
10. Briefly put the tube on ice to cool it down.
11. Set up a PCR reaction as follows (values per reaction):
    - 16.4 μl Nuclease-free water
    - 5 μl 5x Buffer
    - 1.1 μl dNTP
    - 0.75 μl LongAmp Taq-polymerase
    - 4 μl Tagmented DNA
    - 0.75 μl RLB (01–12 A, at 10 μM)
12. Mix gently by flicking the tube, and spin down.
13. Amplify using the following cycling conditions:
    - Initial denaturation 3 min @ 95 °C (1 cycle)
    - Denaturation 15 s @ 95 °C (14 cycles)
    - Annealing 15 s @ 56 °C (14 cycles)
    - Extension 6 min @ 65 °C (14 cycles)
    - Final extension 6 min @ 65 °C (1 cycle)
    - Hold ∼ @ 4 °C
14. Prepare for sample cleaning and concentration:
    a) Resuspend the AMPure XP beads, shake vigorously for at least 30 s.
    b) Prepare 1000 μl of fresh 70% ethanol in MQ per library +100 μl spare
15. Transfer 15 μl of each sample (12 barcoded samples in one library) to a clean 2 ml tube. Spare the rest in cold room until acceptable result from sequencing is obtained.
    a) The volume of pooled library should be 180 μl
    b) If there are fewer samples than 12, increase the volume of the samples to be 60 μl or adjust the volumes of beads and ethanol in step 16.
16. Add 324 μl of resuspended AMPure XP beads (1.8x sample volume) and 1276 μl of 100% ethanol (end concentration of ethanol 70%) to the reaction and mix by pipetting.
    a) Incubate on a mixer for 15 min at +4 °C (cold room shaker, speed 20 rpm).
    b) Keep tubes horizontal
    c) Beads should look clumpy by the end of the incubation. If homogenous, leave for another 10 min
18. Spin down the sample and pellet on a magnet. Keep the tube on the magnet, and pipette off the supernatant.
19. Keep the tube on the magnet and wash the beads with 200 μl of freshly prepared 75% ethanol without disturbing the pellet. Remove the ethanol using a pipette and discard.
20. Repeat the previous step.
21. Spin down and place the tube back on the magnet.
22. Pipette off any residual ethanol. Allow drying for ∼60 s.
23. Remove the tube from the magnetic rack and resuspend pellet in 15 μl of 10 mM Tris-HCl pH 8.0 with 50 mM NaCl.
24. Incubate for 10 min at RT.
25. Pellet the beads on a magnet until the eluate is clear and colourless.
26. Remove and retain the eluate which contains the DNA in a clean 1.5 ml tube. Dispose of the pelleted beads
27. Quantify 1 μl of eluted sample using a Nanopore spectrophotometer.
    - The optimal concentration is 200–400 ng/μl, the bare minimum is 160 ng/μl
28. Take 10 μl of the library into a separate tube.
29. Add 1 μl of RAP to the barcoded DNA.
30. Mix gently by flicking the tube, and spin down.
31. Incubate the reaction for 5 min at RT
32. Keep on ice until ready to load.
33. Prime the flow cell according to the Nanopore protocol.

13. Annex 4. Sequence data characteristics

Table A 1
Comparison in abundance of the identified species produced with Pavian. The taxonomic ranks are domain (D), kingdom (K), phylum (P), class (C), order (O), family (F), genus (G) and species (S). Taxonomic IDs are assigned according to NCBI taxonomy database on 17.2 2022. Abundancy among assembled contigs is presented as percentage of the total number.

Name	Rank	Taxonomic ID	Biospot	Burkard	Rapid-E
Acinetobacter calcoaceticus/baumannii complex > Acinetobacter seifertii	S	1 530 123	0.35%		0.23%
Archaea> … >Methanosarcina mazei	S	2209	0.35%		
Bacteria	D	2	11.19%	3.80%	17.32%
Burkholderiales> … >Ralstonia pickettii 12 J	–	402 626			0.03%
cellular organisms	–	131 567	44.06%	41.14%	43.39%
Cellulosimicrobium cellulans	S	1710			1.18%
Cellulosimicrobium sp. BI34T	S	2 587 808			0.03%
Cellulosimicrobium sp. JZ28	S	1 906 273			0.05%
Cellulosimicrobium sp. TH-20	S	1 980 001			0.05%
Chromatiales> … >Thioalkalivibrio sulfidiphilus HL-EbGr7	–	396 588		0.05%	
Enterobacterales	O	91 347	10.84%	3.61%	13.48%
Enterobacteriaceae	F	543	10.84%	3.61%	13.40%
Erwiniaceae > Erwinia	G	551			0.03%
Escherichia coli K-12>*Escherichia coli* BW2952	–	595 496		0.05%	0.31%
Escherichia coli KO11FL	–	595 495	0.35%	0.35%	1.36%
Escherichia coli SE11	–	409 438		0.20%	0.72%
Escherichia coli UMNF18	–	1 050 617			0.08%
Escherichia > *Escherichia coli*	S	562	0.70%	0.79%	4.15%
Escherichia > Escherichia marmotae	S	1 499 973			0.03%
eudicotyledons> … >Arachis	G	3817			0.03%
eudicotyledons> … >Cajanus cajan	S	3821		0.05%	
eudicotyledons> … >Capsicum annuum	S	4072			0.05%
eudicotyledons> … >Cynara cardunculus var. scolymus	–	59 895			0.03%
eudicotyledons> … >Glycine subgen. Soja	–	1 462 606			0.03%
eudicotyledons> … >Gossypium arboreum	S	29 729			0.05%
eudicotyledons> … >Gossypium raimondii	S	29 730		0.05%	
eudicotyledons> … >Helianthus annuus	S	4232		0.05%	0.03%
eudicotyledons> … >Juglans regia	S	51 240			0.03%
eudicotyledons> … >Phaseolus vulgaris	S	3885		0.05%	
eudicotyledons> … >Quercus lobata	S	97 700			0.03%
eudicotyledons> … >Rosa chinensis	S	74 649			0.03%
eudicotyledons> … >Vigna	G	3913	0.35%		
Eukaryota	D	2759	32.52%	37.33%	25.94%
FCB group> … >Chryseobacterium haifense	S	421 525			0.03%
FCB group> … >Flavobacterium faecale	S	1 355 330			0.08%
FCB group> … >Pedobacter sp. HDW13	S	2 714 940			0.03%
Klebsiella > *Klebsiella pneumoniae*	S	573		0.05%	
Liliopsida> … >Brachypodium distachyon	S	15 368			0.03%
Liliopsida> … >Triticum dicoccoides	S	85 692			0.05%
Opisthokonta> … >*Homo sapiens*	S	9606	32.17%	37.09%	25.45%
Opisthokonta> … >*Saccharomyces cerevisiae* S288C	–	559 292			0.03%
Opisthokonta> … >Saccharomyces eubayanus	S	1 080 349			0.05%
other entries > other sequences	–	28 384		0.10%	0.18%
Pectobacteriaceae > Brenneria > Brenneria goodwinii	S	1 109 412			0.03%
Proteobacteria> … >Bradyrhizobium sp. ORS 285	S	115 808			0.03%
Proteobacteria> … >Sinorhizobium	G	28 105			0.03%
Proteobacteria > Alphaproteobacteria > Sphingomonadales	O	204 457			0.05%
Proteobacteria > Betaproteobacteria	C	28 216		0.05%	0.03%
Proteobacteria > Gammaproteobacteria	C	1236	11.19%	3.70%	14.17%
Pseudomonadales > Moraxellaceae > Acinetobacter	G	469	0.35%		0.26%
Pseudomonadales > Pseudomonadaceae > Pseudomonas	G	286		0.05%	0.31%
Pseudomonas fluorescens group > Pseudomonas fluorescens	S	294			0.03%
Ranunculales> … >Papaver somniferum	S	3469		0.05%	
Root	–	1	59.44%	45.19%	57.66%
Salmonella > *Salmonella enterica*	S	28 901	0.35%	0.15%	0.38%
Shigella	G	620	9.79%	2.62%	8.64%
Shigella flexneri	S	623	9.79%	2.62%	8.36%
Sphingomonadaceae> … >Sphingomonas sp. HMP9	S	1 517 554			0.03%
Terrabacteria group> … >Bacillus smithii	S	1479			0.03%
Terrabacteria group> … >Blastococcus saxobsidens DD2	–	1 146 883			0.03%
Terrabacteria group> … >Cellulosimicrobium	G	157 920			2.67%
Terrabacteria group> … >Cutibacterium acnes	S	1747			0.03%
Terrabacteria group> … >Enterococcus faecium	S	1352			0.03%
Terrabacteria group> … >Leuconostoc	G	1243			0.03%
Terrabacteria group> … >Oenococcus oeni	S	1247			0.03%
Terrabacteria group> … >Salinibacterium sp. dk2585	S	2 603 292			0.03%
Terrabacteria group> … >Streptomycetaceae	F	2062			0.03%
Unclassified	U	0	40.56%	54.81%	42.34%
unclassified Cellulosimicrobium	–	2 624 466			0.15%
Viridiplantae> … >Mesangiospermae	–	1 437 183	0.35%	0.25%	0.38%

References

Afshinnekoo, E., Meydan, C., Chowdhury, S., Jaroudi, D., Boyer, C., Bernstein, N., Maritz, J.M., Reeves, D., Gandara, J., Chhangawala, S., Ahsanuddin, S., Simmons, A., Nessel, T., Sundaresh, B., Pereira, E., Jorgensen, E., Kolokotronis, S.-O., Kirchberger, N., Garcia, I., Gandara, D., Dhanraj, S., Nawrin, T., Saletore, Y., Alexander, N., Vijay, P., Hénaff, E.M., Zumbo, P., Walsh, M., O'Mullan, G.D., Tighe, S., Dudley, J.T., Dunaif, A., Ennis, S., O'Halloran, E., Magalhaes, T.R., Boone, B., Jones, A.L., Muth, T.R., Paolantonio, K.S., Alter, E., Schadt, E.E., Garbarino, J., Prill, R.J., Carlton, J.M., Levy, S., Mason, C.E., 2015. Geospatial resolution of human and bacterial diversity with city-scale metagenomics. Cell Syst. 1, 72–87. https://doi.org/10.1016/j.cels.2015.01.001.

Banchi, E., Ametrano, C.G., Stanković, D., Verardo, P., Moretti, O., Gabrielli, F., Lazzarin, S., Borney, M.F., Tassan, F., Tretiach, M., Pallavicini, A., Muggia, L., 2018. DNA metabarcoding uncovers fungal diversity of mixed airborne samples in Italy. PLoS One 13, e0194489. https://doi.org/10.1371/journal.pone.0194489.

Banchi, E., Ametrano, C.G., Tordoni, E., Stanković, D., Ongaro, S., Tretiach, M., Pallavicini, A., Muggia, L., Verardo, P., Tassan, F., Trobiani, N., Moretti, O., Borney, M.F., Lazzarin, S., 2020. Environmental DNA assessment of airborne plant and fungal seasonal diversity. Sci. Total Environ. 738, 140249 https://doi.org/10.1016/j.scitotenv.2020.140249.

Bell, K.L., Burgess, K.S., Botsch, J.C., Dobbs, E.K., Read, T.D., Brosi, B.J., 2019. Quantitative and qualitative assessment of pollen DNA metabarcoding using constructed species mixtures. Mol. Ecol. 28, 431–455. https://doi.org/10.1111/mec.14840.

Berensmeier, S., 2006. Magnetic particles for the separation and purification of nucleic acids. Appl. Microbiol. Biotechnol. 73, 495–504. https://doi.org/10.1007/s00253-006-0675-0.

Brasseur, G.P., Xie, Y., Petersen, A.K., Bouarar, I., Flemming, J., Gauss, M., Jiang, F., Kouznetsov, R., Kranenburg, R., Mijling, B., Peuch, V.-H., Pommier, M., Segers, A., Sofiev, M., Timmermans, R., van der A, R., Walters, S., Xu, J., Zhou, G., 2019. Ensemble forecasts of air quality in eastern China – Part 1: model description and implementation of the MarcoPolo–Panda prediction system, version 1. Geosci. Model Dev. 12, 33–67. https://doi.org/10.5194/gmd-12-33-2019.

Breitwieser, F.P., Salzberg, S.L., 2020. Pavian: interactive analysis of metagenomics data for microbiomics and pathogen identification. Bioinformatics 36, 1303–1304. https://doi.org/10.1093/bioinformatics/btz715.

Brennan, G., Potter, C., Adams-Groom, B., Barber, A., Clewlow, Y., De Vere, N., Griffith, G., Hanlon, H., Hegarty, M., Kurgancky, A., Mc Innes, R., Petch, G., Osborne, N., Skjoth, C., Wheeler, B., Creer, S., 2019. Assessing Quantitative Taxon-specific Grass Pollen Biodiversity in Time and Space Using Targeted Molecular Analysis of Aerial Environmental DNA. Wiley, pp. 39–40. https://doi.org/10.1111/all.13957. Presented at the EAACI Symposium 2019.

Buters, J.T.M., Antunes, C., Galveias, A., Bergmann, K.C., Thibaudon, M., Galán, C., Schmidt-Weber, C., Oteros, J., 2018. Pollen and spore monitoring in the world. Clin. Transl. Allergy 8, 9. https://doi.org/10.1186/s13601-018-0197-8.

Cao, S., Zhang, W., Ding, W., Wang, Meng, Fan, S., Yang, B., Mcminn, A., Wang, Min, Xie, B., Qin, Q.-L., Chen, X.-L., He, J., Zhang, Y.-Z., 2020. Structure and function of the Arctic and Antarctic marine microbiota as revealed by metagenomics. Microbiome 8, 47. https://doi.org/10.1186/s40168-020-00826-9.

Carslaw, K.S., Luo, B., Peter, T., 1995. An analytic expression for the composition of aqueous HNO $_3$ -H $_2$ SO $_4$ stratospheric aerosols including gas phase removal of HNO $_3$. Geophys. Res. Lett. 22, 1877–1880. https://doi.org/10.1029/95GL01668.

Cecchi, L., D'Amato, G., Ayres, J.G., Galan, C., Forastiere, F., Forsberg, B., Gerritsen, J., Nunes, C., Behrendt, H., Akdis, C., Dahl, R., Annesi-Maesano, I., 2010. Projections of the effects of climate change on allergic asthma: the contribution of aerobiology. Allergy 65, 1073–1081. https://doi.org/10.1111/j.1398-9995.2010.02423.x.

Clot, B., Gilge, S., Hajkova, L., Magyar, D., Scheifinger, H., Sofiev, M., Bütler, F., Tummon, F., 2020. The EUMETNET AutoPollen Programme: Establishing a Prototype Automatic Pollen Monitoring Network in Europe. Aerobiologia. https://doi.org/10.1007/s10453-020-09666-4.

Creamean, J.M., Suski, K.J., Rosenfeld, D., Cazorla, A., DeMott, P.J., Sullivan, R.C., White, A.B., Ralph, F.M., Minnis, P., Comstock, J.M., Tomlinson, J.M., Prather, K.A., 2013. Dust and biological aerosols from the Sahara and Asia influence precipitation in the western U.S. Science 339, 1572–1578. https://doi.org/10.1126/science.1227279.

Crouzy, B., Stella, M., Konzelmann, T., Calpini, B., Clot, B., 2016. All-optical automatic pollen identification: towards an operational system. Atmos. Environ. 140, 202–212. https://doi.org/10.1016/j.atmosenv.2016.05.062.

D'Amato, G., Cecchi, L., Bonini, S., Nunes, C., Liccardi, G., Popov, T., Cauwenberge, P.V., 2007. Allergenic Pollen and Pollen Allergy in Europe. https://doi.org/10.1111/j.1398-9995.2007.01393.x. Allergy 976–990.

Damski, J., Thölix, L., Backman, L., Taalas, P., Kulmala, M., 2007. FinROSE — middle atmospheric chemistry transport model. Boreal Environ. Res. 12, 535–550.

Danko, D., Bezdan, D., Afshin, E.E., Ahsanuddin, S., Bhattacharya, C., Butler, D.J., Chng, K.R., Donnellan, D., Hecht, J., Jackson, K., Kuchin, K., Karasikov, M., Lyons, A., Mak, L., Meleshko, D., Mustafa, H., Mutai, B., Neches, R.Y., Ng, A., Nikolayeva, O., Nikolayeva, T., Png, E., Ryon, K.A., Sanchez, J.L., Shaaban, H., Sierra, M.A., Thomas, D., Young, B., Abudayyeh, O.O., Alicea, J., Bhattacharyya, M., Blekhman, R., Castro-Nallar, E., Cañas, A.M., Chatziefthimiou, A.D., Crawford, R.W., De Filippis, F., Deng, Y., Desnues, C., Dias-Neto, E., Dybwad, M., Elhaik, E., Ercolini, D., Frolova, A., Gankin, D., Gootenberg, J.S., Graf, A.B., Green, D.C., Hajirasouliha, I., Hastings, J.J.A., Hernandez, M., Iraola, G., Jang, S., Kahles, A., Kelly, F.J., Knights, K., Kyrpides, N.C., Łabaj, P.P., Lee, P.K.H., Leung, M.H.Y., Ljungdahl, P.O., Mason-Buck, G., McGrath, K., Meydan, C., Mongodin, E.F., Moraes, M.O., Nagarajan, N., Nieto-Caballero, M., Noushmehr, H., Oliveira, M., Ossowski, S., Osuolale, O.O., Özcan, O., Paez-Espino, D., Rascovan, N., Richard, H., Rätsch, G., Schriml, L.M., Semmler, T., Sezerman, O.U., Shi, L., Shi, T., Siam, R., Song, L.H., Suzuki, H., Court, D.S., Tighe, S.W., Tong, X., Udekwu, K.I., Ugalde, J.A., Valentine, B., Vassilev, D.I., Vayndorf, E.M., Velavan, T.P., Wu, J., Zambrano, M.M., Zhu, J., Zhu, S., Mason, C.E., Abdullah, N., Abraao, M., Adel, A., Afaq, M., Al-Quaddoomi, F.S., Alam, I., Albuquerque, G.E., Alexiev, A., Ali, K., Alvarado-Arnez, L. E., Aly, S., Amachee, J., Amorim, M.G., Ampadu, M., Amran, M.A.-F., An, N., Andrew, W., Andrianjakarivony, H., Angelov, M., Antelo, V., Aquino, C., Aranguren, Á., Araujo, L.F., Vasquez Arevalo, H.F., Arevalo, J., Arnan, C., Alvarado Arnez, L.E., Arredondo, F., Arthur, M., Asenjo, F., Aung, T.S., Auvinet, J., Aventin, N., Ayaz, S., Baburyan, S., Bakere, A.-M., Bakhl, K., Bartelli, T.F., Batdelger, E., Baudon, F., Becher, K., Bello, C., Benchouaia, M., Benisty, H., Benoiston, A.-S., Benson, J., Benítez, D., Bernardes, J., Bertrand, D., Beurmann, S., Bitard-Feildel, T., Bittner, L., Black, C., Blanc, G., Blyther, B., Bode, T., Boeri, J., Boldgiv, B., Bolzli, K., Bordigoni, A., Borrelli, C., Bouchard, S., Bouly, J.-P., Boyd, A., Branco, G.P., Breschi, A., Brindefalk, B., Brion, C., Briones, A., Buczansla, P., Burke, C.M., Burrell, A., Butova, A., Buttar, I., Bynoe, J., Bönigk, S., Bøifot, K.O., Caballero, H., Cai, X.W., Calderon, D., Cantillo, A., Carbajo, M., Carbone, A., Cardenas, A., Carrillo, K., Casalot, L., Castro, S., Castro, A.V., Castro, A., Castro, A.V. B., Cawthorne, S., Cedillo, J., Chaker, S., Chalangal, J., Chan, A., Chasapi, A.I., Chatziefthimiou, S., Chaudhuri, S.R., Chavan, A.K., Chavez, F., Chem, G., Chen, X., Chen, M., Chen, J.-W., Chernomoretz, A., Chettouh, A., Cheung, D., Chicas, D., Chiu, S., Choudhry, H., Chrispin, C., Ciaramella, K., Cifuentes, E., Cohen, J., Coil, D. A., Collin, S., Conger, C., Conte, R., Corsi, F., Cossio, C.N., Costa, A.F., Cuebas, D., D'Alessandro, B., Dahlhausen, K.E., Darling, A.E., Das, P., Davenport, L.B., David, L., Davidson, N.R., Dayama, G., Delmas, S., Deng, C.K., Dequeker, C., Desert, A., Devi, M., Dezem, F.S., Dias, C.N., Donahoe, T.R., Dorado, S., Dorsey, L., Dotsenko, V., Du, S., Dutan, A., Eady, N., Eisen, J.A., Elaskandrany, M., Epping, L., Escalera-Antezana, J.P., Ettinger, C.L., Faiz, I., Fan, L., Farhat, N., Faure, E., Fauzi, F., Feigin, C., Felice, S., Ferreira, L.P., Figueroa, G., Fleiss, A., Flores, D., Velasco, Flores, J.L., Fonseca, M.A.S., Foox, J., Forero, J.C., Francis, A., French, K., Fresia, P., Friedman, J., Fuentes, J.J., Galipon, J., Garcia, M., Garcia, L., García, C., Geiger, A., Gerner, S.M., Ghose, S.L., Giang, D.P., Giménez, M., Giovannelli, D., Githae, D., Gkotzis, S., Godoy, L., Goldman, S., Gonnet, G.H., Gonzalez, J., Gonzalez, A., Gonzalez-Poblete, C., Gray, A., Gregory, T., Greselle, C., Guasco, S., Guerra, J., Gurianova, N., Haehr, W., Halary, S., Hartkopf, F., Hastings, J.J.A., Hawkins-Zafarnia, A., Hazrin-Chong, N.H., Helfrich, E., Hell, E., Henry, T., Hernandez, S., Hernandez, P.L., Hess-Homeier, D., Hittle, L.E., Hoan, N.X., Holik, A., Homma, C., Hoxie, I., Huber, M., Humphries, E., Hyland, S., Hässig, A., Häusler, R., Hüsser, N., Petit, R.A., Iderzorig, B., Igarashi, M., Iqbal, S.B., Ishikawa, S., Ishizuka, S., Islam, S., Islam, R., Ito, K., Ito, S., Ito, T., Ivankovic, T., Iwashiro, T., Jackson, S., Jacobs, J., James, M., Jaubert, M., Jerier, M.-L., Jiminez, E., Jinfessa, A., De Jong, Y., Joo, H.W., Jospin, G., Kajita, T., Ahmad Kassim, A.S., Kato, N., Kaur, A., Kaur, I., de Souza Gomes Kehdy, F., Khadka, V.S., Khan, S., Khavari, M., Ki, M., Kim, G., Kim, H.J., Kim, S., King, R.J., Knights, K., KoLoMonaco, G., Koag, E., Kobko-Litskevitch, N., Korshevniuk, M., Kozhar, M., Krebs, J., Kubota, N., Kuklin, A., Kumar, S.S., Kwong, R., Kwong, L., Lafontaine, I., Lago, J., Lai, T.Y., Laine, E., Laiola, M., Lakhneko, O., Lamba, I., de Lamotte, G., Lannes, R., De Lazzari, E., Leahy, M., Lee, H., Lee, Y., Lee, L., Lemaire, V., Leong, E., Leung, M.H.Y., Lewandowska, D., Li, C., Liang, W., Lin, M., Lisboa, P., Litskevitch, A., Liu, E.M., Liu, T., Livia, M.A., Lo, Y.H., Losim, S., Loubens, M., Lu, J., Lykhenko, O., Lysakova, S., Mahmoud, S., Majid, S.A., Makogon, N., Maldonado, D., Mallari, K., Malta, T.M., Mamun, M., Manoir, D., Marchandon, G., Marciniak, N., Marinovic, S., Marques, B., Mathews, N., Matsuzaki, Y., Matthys, V., May, M., McComb, E., Meagher, A., Melamed, A., Menary, W., Mendez, K.N., Mendez, A., Mendy, I.M., Meng, I., Menon, A., Menor, M., Meoded, R., Merino, N., Meydan, C., Miah, K., Mignotte, M., Miketic, T., Miranda, W., Mitsios, A., Miura, R., Miyake, K., Moccia, M. D., Mohan, N., Mohsin, M., Moitra, K., Moldes, M., Molina, L., Molinet, J., Molomjamts, O.-E., Moniruzzaman, E., Moon, S., de Oliveira Moraes, I., Moreno, M., Mosella, M.S., Moser, J.W., Mozsary, C., Muehlbauer, A.L., Muner, O., Munia, M., Munim, N., Muscat, M., Mustac, T., Muñoz, C., Nadalin, F., Naeem, A., Nagy-Szakal, D., Nakagawa, M., Narce, A., Nasu, M., Navarrete, I.G., Naveed, H., Nazario, B., Nedunuri, N.R., Neff, T., Nesimi, A., Ng, W.C., Ng, S., Nguyen, G., Ngwa, E., Nicolas, A., Nicolas, P., Nika, A., Noorzi, H., Nosrati, A., Noushmehr, H., Nunes, D.N., O'Brien, K., O'Hara, N.B., Oken, G., Olawoyin, R.A., Oliete, J.Q., Olmeda, K., Oluwadare, T., Oluwadare, I.A., Ordioni, N., Orpilla, J., Orrego, J., Ortega, M., Osma, P., Osuolale, I.O., Osuolale, O.M., Ota, M., Oteri, F., Oto, Y., Ounit, R., Ouzounis, C.A., Pakrashi, S., Paras, R., Pardo-Este, C., Park, Y.-J., Pastuszek, P., Patel, S., Pathmanathan, J., Patrignani, A., Perez, M., Peros, A., Persaud, S., Peters, A., Phillips, A., Pineda, L., Pizzi, M.P., Plaku, Alma, Plaku, Alketa, Pompa-Hogan, B., Portilla, M.G., Posada, L., Priestman, M., Prithiviraj, B., Priya, S., Pugdeethosal, P., Pugh, C.E., Pulatov, B., Pupiec, A., Pyrshev, K., Qing, T., Rahiel, S., Rahmatulloev, S., Rajendran, K., Ramcharan, A., Ramirez-Rojas, A., Rana, S., Ratnanandan, P., Read, T.D., Rehrauer, H., Richer, R., Rivera, A., Rivera, M., Robertiello, A., Robinson, C., Rodríguez, P., Rojas, N.A., Roldán, P., Rosario, A., Roth, S., Ruiz, M., Boja Ruiz, S.E., Russell, K., Rybak, M., Sabedot, T.S., Sabina, M., Saito, I., Saito, Y., Malca Salas, G.A., Salazar, C., San, K.M., Sanchez, J., Sanchir, K., Sankar, R., de Souza Santos, P.T., Saravi, Z., Sasaki, K., Sato, Y., Sato, M., Sato, S., Sato, R., Sato, K., Sayara, N., Schaaf, S., Schacher, O., Schinke, A.-L.M., Schlapbach, R., Schori, C., Schriml, J.R., Segato, F., Sepulveda, F., Serpa, M.S., De Sessions, P.F., Severyn, J.C., Shaaban, H., Shakil, M., Shalaby, S., Shari, A., Shim, H., Shirahata, H., Shiwa, Y., Siam, R., Da Silva, O., Silva, J.M., Simon, G., Singh, S.K., Sluzek, K., Smith, R., So, E., Andreu Somavilla, N., Sonohara, Y., Rufino de Sousa, N., Souza, C., Sperry, J., Sprinsky, N., Stark, S.G., La Storia, A., Suganuma, K., Suliman, H., Sullivan, J., Supie, A.A.M., Suzuki, C., Takagi, S., Takahara, F., Takahashi, N., Takahashi, K., Takeda, T., Takenaka, I.K.,

Tanaka, S., Tang, A., Man Tang, Y., Tarcitano, E., Tassinari, A., Taye, M., Terrero, A., Thambiraja, E., Thiébaut, A., Thomas, S., Thomas, A.M., Togashi, Y., Togashi, T., Tomaselli, A., Tomita, M., Tomita, I., Tong, X., Toth, O., Toussaint, N.C., Tran, J.M., Truong, C., Tsonev, S.I., Tsuda, K., Tsurumaki, T., Tuz, M., Tymoshenko, Y., Urgiles, C., Usui, M., Vacant, S., Valentine, B., Vann, L.E., Velter, F., Ventorino, V., Vera-Wolf, P., Vicedomini, R., Suarez-Villamil, M.A., Vincent, S., Vivancos-Koopman, R., Wan, A., Wang, C., Warashina, T., Watanabe, A., Weekes, S., Werner, J., Westfall, D., Wieler, L.H., Williams, M., Wolf, S.A., Wong, B., Wong, Y.L., Wong, T., Wright, R., Wunderlin, T., Yamanaka, R., Yang, J., Yano, H., Yeh, G.C., Yemets, O., Yeskova, T., Yoshikawa, S., Zafar, L., Zhang, Y., Zhang, S., Zhang, A., Zheng, Y., Zubenko, S., 2021. A global metagenomic map of urban microbiomes and antimicrobial resistance. Cell 184, 3376–3393. https://doi.org/10.1016/j.cell.2021.05.002 e17.

de Araujo, G.G., Rodrigues, F., Gonçalves, F.L.T., Galante, D., 2019. Survival and ice nucleation activity of Pseudomonas syringae strains exposed to simulated high-altitude atmospheric conditions. Sci. Rep. 9, 7768. https://doi.org/10.1038/s41598-019-44283-3.

del Campo, J., Sieracki, M.E., Molestina, R., Keeling, P., Massana, R., Ruiz-Trillo, I., 2014. The others: our biased perspective of eukaryotic genomes. Trends Ecol. Evol. 29, 252–259. https://doi.org/10.1016/j.tree.2014.03.006.

Delort, A.-M., Amato, P. (Eds.), 2017. Microbiology of Aerosols. John Wiley & Sons, Hoboken, NJ.

Després, VivianeR., Huffman, J.A., Burrows, S.M., Hoose, C., Safatov, AleksandrS., Buryak, G., Fröhlich-Nowoisky, J., Elbert, W., Andreae, MeinratO., Pöschl, U., Jaenicke, R., 2012. Primary biological aerosol particles in the atmosphere: a review. Tellus B 64, 15598. https://doi.org/10.3402/tellusb.v64i0.15598.

Fröhlich-Nowoisky, J., 2016. Bioaerosols in the Earth system: climate, health, and ecosystem interactions. Atmos. Res. 182, 346–376.

Galán, C., Smith, M., Thibaudon, M., Frenguelli, G., Oteros, J., Gehrig, R., Berger, U., Clot, B., Brandao, R., Group, E.Q.W., 2014. Pollen monitoring: minimum requirements and reproducibility of analysis. Aerobiologia 30, 385–395.

Gallagher, S., 1998. Quantitation of nucleic acids with absorption spectroscopy. In: Coligan, J.E., Dunn, B.M., Speicher, D.W., Wingfield, P.T. (Eds.), Current Protocols in Protein Science. John Wiley & Sons, Inc., Hoboken, NJ, USA, pp. A.4K.1–A.4K.3. https://doi.org/10.1002/0471140864.psa04ks13.

Garlapati, D., Charankumar, B., Ramu, K., Madeswaran, P., Ramana Murthy, M.V., 2019. A review on the applications and recent advances in environmental DNA (eDNA) metagenomics. Rev. Environ. Sci. Biotechnol. 18, 389–411. https://doi.org/10.1007/s11157-019-09501-4.

Gery, M.W., Whitten, G.Z., Killus, J.P., Dodge, M.C., 1989. A photochemical kinetics mechanism for urban and regional scale computer modelling. J. Geophys. Res.-Atmos. 94, 12925–12956 https://doi.org/0148-0227/89/89JD-00793$05.00.

Glasel, J.A., 1995. Validity of nucleic acid purities monitored by 260nm/280nm absorbance ratios. Biotechniques 18, 62–63.

Guxens, M., Ghassabian, A., Gong, T., Garcia-Esteban, R., Porta, D., Giorgis-Allemand, L., Almqvist, C., Aranbarri, A., Beelen, R., Badaloni, C., Cesaroni, G., de Nazelle, A., Estarlich, M., Forastiere, F., Forns, J., Gehring, U., Ibarluzea, J., Jaddoe, V.W.V., Korek, M., Lichtenstein, P., Nieuwenhuijsen, M.J., Rebagliato, M., Slama, R., Tiemeier, H., Verhulst, F.C., Volk, H.E., Pershagen, G., Brunekreef, B., Sunyer, J., 2016. Air pollution exposure during pregnancy and childhood autistic traits in four European population-based cohort studies: the ESCAPE project. Environ. Health Perspect. 124, 133–140. https://doi.org/10.1289/ehp.1408483.

Hajibabaei, M., Singer, G.A.C., Hebert, P.D.N., Hickey, D.A., 2007. DNA barcoding: how it complements taxonomy, molecular phylogenetics and population genetics. Trends Genet. 23, 167–172. https://doi.org/10.1016/j.tig.2007.02.001.

Harrison, S.T.L., 1991. Bacterial cell disruption: a key unit operation in the recovery of intracellular products. Biotechnol. Adv. 9, 217–240. https://doi.org/10.1016/0734-9750(91)90005-G.

Hervàs, A., Camarero, L., Reche, I., Casamayor, E.O., 2009. Viability and potential for immigration of airborne bacteria from Africa that reach high mountain lakes in Europe. Environ. Microbiol. 11, 1612–1623. https://doi.org/10.1111/j.1462-2920.2009.01926.x.

Hirst, J.M., 1952. An automatic volumetric spore trap. Ann. Appl. Biol. 39, 257–265. https://doi.org/10.1111/j.1744-7348.1952.tb00904.x.

Hsu, T., Joice, R., Vallarino, J., Abu-Ali, G., Hartmann, E.M., Shafquat, A., DuLong, C., Baranowski, C., Gevers, D., Green, J.L., Morgan, X.C., Spengler, J.D., Huttenhower, C., 2016. Urban transit system microbial communities differ by surface type and interaction with humans and the environment. mSystems 1, e00018-16. https://doi.org/10.1128/mSystems.00018-16.

Huffman, J.A., Perring, A.E., Savage, N.J., Clot, B., Crouzy, B., Tummon, F., Shoshanim, O., Damit, B., Schneider, J., Sivaprakasam, V., Zawadowicz, M.A., Crawford, I., Gallagher, M., Topping, D., Doughty, D.C., Hill, S.C., Pan, Y., 2019. Real-time sensing of bioaerosols: review and current perspectives. Aerosol. Sci. Technol. 1–31. https://doi.org/10.1080/02786826.2019.1664724.

Huijnen, V., Eskes, H.J., Poupkou, A., Elbern, H., Boersma, K.F., Foret, G., Sofiev, M., Valdebenito, A., Flemming, J., Stein, O., Gross, A., Robertson, L., D'Isidoro, M., Kioutsioukis, I., Friese, E., Amstrup, B., Bergstrom, R., Strunk, A., Vira, J., Zyryanov, D., Maurizi, A., Melas, D., Peuch, V.-H., Zerefos, C., 2010. Comparison of OMI NO2 tropospheric columns with an ensemble of global and European regional air quality models. Atmos. Chem. Phys. 10, 3273–3296.

Humbal, C., Gautam, S., Trivedi, U., 2018. A review on recent progress in observations, and health effects of bioaerosols. Environ. Int. 118, 189–193. https://doi.org/10.1016/j.envint.2018.05.053.

Jäger, S., Mandroli, P., Spieksma, F., Emberlin, J., Hjelmroos, M., Rantio-Lehtimaki, A., Al, E., 1995. News. Aerobiol. 11, 69–70.

Ji, Y., Ashton, L., Pedley, S.M., Edwards, D.P., Tang, Y., Nakamura, A., Kitching, R., Dolman, P.M., Woodcock, P., Edwards, F.A., Larsen, T.H., Hsu, W.W., Benedick, S., Hamer, K.C., Wilcove, D.S., Bruce, C., Wang, X., Levi, T., Lott, M., Emerson, B.C., Yu, D.W., 2013. Reliable, verifiable and efficient monitoring of biodiversity via metabarcoding. Ecol. Lett. 16, 1245–1257. https://doi.org/10.1111/ele.12162.

Joly, S., Davies, T.J., Archambault, A., Bruneau, A., Derry, A., Kembel, S.W., Peres-Neto, P., Vamosi, J., Wheeler, T.A., 2014. Ecology in the age of DNA barcoding: the resource, the promise and the challenges ahead. Mol. Ecol. Resour. 14, 221–232. https://doi.org/10.1111/1755-0998.12173.

Jorquera, H., Borzutzky, A., Hoyos-Bachiloglu, R., García, A., 2015. Association of Kawasaki disease with tropospheric winds in Central Chile: is wind-borne desert dust a risk factor? Environ. Int. 78, 32–38. https://doi.org/10.1016/j.envint.2015.02.007.

Kanji, Z.A., Ladino, L.A., Wex, H., Boose, Y., Burkert-Kohn, M., Cziczo, D.J., Krämer, M., 2017. Overview of ice nucleating particles. Meteorol. Monogr. 58, 1.1–1.33. https://doi.org/10.1175/AMSMONOGRAPHS-D-16-0006.1.

Katevatis, C., Fan, A., Klapperich, C.M., 2017. Low concentration DNA extraction and recovery using a silica solid phase. PLoS One 12, e0176848. https://doi.org/10.1371/journal.pone.0176848.

Korhonen, H., Carslaw, K.S., Spracklen, D.V., Mann, G.W., Woodhouse, M.T., 2008. Influence of oceanic dimethyl sulfide emissions on cloud condensation nuclei concentrations and seasonality over the remote Southern Hemisphere oceans: a global model study. J. Geophys. Res. 113, D15204 https://doi.org/10.1029/2007JD009718.

Kouznetsov, R., Sofiev, M., 2012. A methodology for evaluation of vertical dispersion and dry deposition of atmospheric aerosols. J. Geophys. Res. 117 https://doi.org/10.1029/2011JD016366.

Kouznetsov, R., Sofiev, M., Vira, J., Stiller, G., 2020. Simulating age of air and the distribution of SF_6 in the stratosphere with the SILAM model. Atmos. Chem. Phys. 20, 5837–5859. https://doi.org/10.5194/acp-20-5837-2020.

Kraaijeveld, K., de Weger, L.A., Ventayol García, M., Buermans, H., Frank, J., Hiemstra, P.S., den Dunnen, J.T., 2015. Efficient and sensitive identification and quantification of airborne pollen using next-generation DNA sequencing. Mol. Ecol. Resour. 15, 8–16. https://doi.org/10.1111/1755-0998.12288.

Kress, W.J., Wurdack, K.J., Zimmer, E.A., Weigt, L.A., Janzen, D.H., 2005. Use of DNA barcodes to identify flowering plants. Proc. Natl. Acad. Sci. USA 102, 8369–8374. https://doi.org/10.1073/pnas.0503123102.

Leggett, R.M., Clark, M.D., 2017. A world of opportunities with nanopore sequencing. J. Exp. Bot. 68, 5419–5429. https://doi.org/10.1093/jxb/erx289.

Li, Y., Chen, S., Liu, N., Ma, L., Wang, T., Veedu, R.N., Li, T., Zhang, F., Zhou, H., Cheng, X., Jing, X., 2020. A systematic investigation of key factors of nucleic acid precipitation toward optimized DNA/RNA isolation. Biotechniques 68, 191–199. https://doi.org/10.2144/btn-2019-0109.

Liao, X., Hu, K., Salhi, A., Zou, Y., Wang, J., Gao, X., 2022. msRepDB: a comprehensive repetitive sequence database of over 80 000 species. Nucleic Acids Res. 50, D236–D245. https://doi.org/10.1093/nar/gkab1089.

Lieberherr, G., Auderset, K., Calpini, B., Clot, B., Crouzy, B., Gysel-Beer, M., Konzelmann, T., Manzano, J., Mihajlovic, A., Moallemi, A., O'Connor, D., Sikoparija, B., Sauvageat, E., Tummon, F., Vasilatou, K., 2021. Assessment of Real-Time Bioaerosol Particle Counters Using Reference Chamber Experiments (Preprint). Aerosols/Laboratory Measurement/Validation and Intercomparisons. https://doi.org/10.5194/amt-2021-136.

Maki, L.R., Galyan, E.L., Chang-Chien, M.-M., Caldwell, D.R., 1974. Ice nucleation induced by *Pseudomonas syringae*. Appl. Microbiol. 28, 456–459. https://doi.org/10.1128/am.28.3.456-459.1974.

Marchuk, G.I., 1995. Adjoint Equations and Analysis of Complex Systems. Kluwer Academic Publisher.

Marcovecchio, F., Perrino, C., 2021. Bioaerosol contribution to atmospheric particulate matter in indoor university environments. Sustainability 13, 1149. https://doi.org/10.3390/su13031149.

Marks, R.A., Hotaling, S., Frandsen, P.B., VanBuren, R., 2021. Representation and participation across 20 years of plant genome sequencing. Native Plants 7, 1571–1578. https://doi.org/10.1038/s41477-021-01031-8.

Martin, M., 2011. Cutadapt removes adapter sequences from high-throughput sequencing reads. EMBnet J. 17, 10. https://doi.org/10.14806/ej.17.1.200.

Mehrotra, S., Goyal, V., 2014. Repetitive sequences in plant nuclear DNA: types, distribution, evolution and function. Dev. Reprod. Biol. 12, 164–171. https://doi.org/10.1016/j.gpb.2014.07.003.

Meinander, O., Kontu, A., Kouznetsov, R., Sofiev, M., 2020. Snow samples combined with long-range transport modeling to reveal the origin and temporal variability of black carbon in seasonal snow in Sodankylä (67°N). Front. Earth Sci. 8, 1–11. https://doi.org/10.3389/feart.2020.00153.

Morris, C.E., Conen, F., Alex Huffman, J., Phillips, V., Pöschl, U., Sands, D.C., 2014. Bioprecipitation: a feedback cycle linking Earth history, ecosystem dynamics and land use through biological ice nucleators in the atmosphere. Global Change Biol. 20, 341–351. https://doi.org/10.1111/gcb.12447.

Núñez, A., Amo de Paz, G., Rastrojo, A., García, A.M., Alcamí, A., Gutiérrez-Bustillo, A. M., Moreno, D.A., 2016. Monitoring of the airborne biological particles in outdoor atmosphere. Part 1: importance, variability and ratios. Int. Microbiol. 1–13. https://doi.org/10.2436/20.1501.01.258.

Oteros, J., Bartusel, E., Alessandrini, F., Núñez, A., Moreno, D.A., Behrendt, H., Schmidt-Weber, C., Traidl-Hoffmann, C., Buters, J., 2019. Artemisia pollen is the main vector for airborne endotoxin. J. Allergy Clin. Immunol. 143, 369–377. https://doi.org/10.1016/j.jaci.2018.05.040 e5.

Oteros, J., Buters, J., Laven, G., Röseler, S., Wachter, R., Schmidt-Weber, C., Hofmann, F., 2017. Errors in determining the flow rate of Hirst-type pollen traps. Aerobiologia 33, 201–210. https://doi.org/10.1007/s10453-016-9467-x.

Oteros, J., Pusch, G., Weichenmeier, I., Heimann, U., Möller, R., Röseler, S., Traidl-Hoffmann, C., Schmidt-Weber, C., Buters, J.T.M., 2015. Automatic and online pollen monitoring. Int. Arch. Allergy Immunol. 167, 158–166. https://doi.org/10.1159/000436968.

Petersen, A.K., Brasseur, G.P., Bouarar, I., Flemming, J., Gauss, M., Jiang, F., Kouznetsov, R., Kranenburg, R., Mijling, B., Peuch, V.-H., Pommier, M., Segers, A., Sofiev, M., Timmermans, R., van der A, R., Walters, S., Xie, Y., Xu, J., Zhou, G., 2019. Ensemble forecasts of air quality in eastern China – Part 2: evaluation of the MarcoPolo–Panda prediction system, version 1. Geosci. Model Dev. 12, 1241–1266. https://doi.org/10.5194/gmd-12-1241-2019.

Poupkou, A., Giannaros, T., Markakis, K., Kioutsioukis, I., Curci, G., Melas, D., Zerefos, C., 2010. A model for European Biogenic Volatile Organic Compound emissions: software development and first validation. Environ. Model. Software 25, 1845–1856. https://doi.org/10.1016/j.envsoft.2010.05.004.

Prank, M., Chapman, D.S., Bullock, J.M., Belmonte, J., Berger, U., Dahl, A., Jäger, S., Kovtunenko, I., Magyar, D., Niemelä, S., Rantio-Lehtimäki, A., Rodinkova, V., Sauliene, I., Severova, E., Sikoparija, B., Sofiev, M., 2013. An operational model for forecasting ragweed pollen release and dispersion in Europe. Agric. For. Meteorol. 182 (183), 43–53. https://doi.org/10.1016/j.agrformet.2013.08.003.

Rojo, J., Núñez, A., Lara, B., Sánchez-Parra, B., Moreno, D.A., Pérez-Badia, R., 2019. Comprehensive analysis of different adhesives in aerobiological sampling using optical microscopy and high-throughput DNA sequencing. J. Environ. Manag. 240, 441–450. https://doi.org/10.1016/j.jenvman.2019.03.116.

Santamaria, M., Fosso, B., Consiglio, A., De Caro, G., Grillo, G., Licciulli, F., Liuni, S., Marzano, M., Alonso-Alemany, D., Valiente, G., Pesole, G., 2012. Reference databases for taxonomic assignment in metagenomics. Briefings Bioinf. 13, 682–695. https://doi.org/10.1093/bib/bbs036.

Šaulienė, I., Šukienė, L., Daunys, G., Valiulis, G., Vaitkevičius, L., Matavulj, P., Brdar, S., Panic, M., Sikoparija, B., Clot, B., Crouzy, B., Sofiev, M., 2019. Automatic pollen recognition with the Rapid-E particle counter: the first-level procedure, experience and next steps. Atmos. Meas. Tech. 12, 3435–3452. https://doi.org/10.5194/amt-12-3435-2019.

Sauvageat, E., Zeder, Y., Auderset, K., Calpini, B., Clot, B., Crouzy, B., Konzelmann, T., Lieberherr, G., Tummon, F., Vasilatou, K., 2020. Real-time pollen monitoring using digital holography. Atmos. Meas. Tech. 13, 1539–1550. https://doi.org/10.5194/amt-13-1539-2020.

Schäfer, J., Weiß, S., Jäckel, U., 2017. Preliminary validation of a method combining cultivation and cloning-based approaches to monitor airborne bacteria. Ann. Work Expos. Health 61, 633–642. https://doi.org/10.1093/annweh/wxx038.

Sevag, M.G., Lackman, D.B., Smolens, J., 1938. The isolation of the components of streptococcal nucleoproteins in serologically active form. J. Biol. Chem. 124, 425–436. https://doi.org/10.1016/S0021-9258(18)74048-9.

Shehadul Islam, M., Aryasomayajula, A., Selvaganapathy, P., 2017. A review on macroscale and microscale cell lysis methods. Micromachines 8, 83. https://doi.org/10.3390/mi8030083.

Sickel, W., Ankenbrand, M.J., Grimmer, G., Holzschuh, A., Härtel, S., Lanzen, J., Steffan-Dewenter, I., Keller, A., 2015. Increased efficiency in identifying mixed pollen samples by meta-barcoding with a dual-indexing approach. BMC Ecol. 15, 20. https://doi.org/10.1186/s12898-015-0051-y.

Soares, J., Sofiev, M., Hakkarainen, J., 2015. Uncertainties of Wild-Land Fires Emission in AQMEII Phase 2 Case Study. Atmospheric Environment. https://doi.org/10.1016/j.atmosenv.2015.01.068.

Sofiev, M., 2019. On possibilities of assimilation of near-real-time pollen data by atmospheric composition models. Aerobiologia 1. https://doi.org/10.1007/s10453-019-09583-1.

Sofiev, M., 2016. On impact of transport conditions on variability of the seasonal pollen index. Aerobiologia 33, 167–179. https://doi.org/10.1007/s10453-016-9459-x.

Sofiev, M., 2002. Extended resistance analogy for construction of the vertical diffusion scheme for dispersion models. J. Geophys. Res.-Atmos. 107 https://doi.org/10.1029/2001JD001233. ACH 10-1-ACH 10-8.

Sofiev, M., 2000. A model for the evaluation of long-term airborne pollution transport at regional and continental scales. Atmos. Environ. 34, 2481–2493.

Sofiev, M., Berger, U., Vira, J., Arteta, J., Belmonte, J., Bergmann, K.-C., Chéroux, F., Elbern, H., Friese, E., Galan, C., Gehrig, R., Khvorostyanov, D., Kranenburg, R., Kumar, U., Marécal, V., Meleux, F., Menut, L., Pessi, A.-M., Robertson, L., Ritenberga, O., Rodinkova, V., Saarto, A., Segers, A., Severova, E., Sauliene, I., Siljamo, P., Steensen, B.M., Teinemaa, E., Thibaudon, M., Peuch, V.-H., 2015a. MACC regional multi-model ensemble simulations of birch pollen dispersion in Europe. Atmos. Chem. Phys. 15, 8115–8130. https://doi.org/10.5194/acp-15-8115-2015.

Sofiev, M., Bergmann, K.-C. (Eds.), 2013. Allergenic Pollen. A Review of Production, Release, Distribution and Health Impact. Springer-Verlag Berlin, Heidelberg.

Sofiev, M., Genikhovich, E., Keronen, P., Vesala, T., 2010. Diagnosing the surface layer parameters for dispersion models within the meteorological-to-dispersion modeling interface. J. Appl. Meteorol. Climatol. 49, 221–233. https://doi.org/10.1175/2009JAMC2210.1.

Sofiev, M., Kouznetsov, R., Hänninen, R., Sofieva, V.F., 2020. Technical note: intermittent reduction of the stratospheric ozone over northern Europe caused by a storm in the Atlantic Ocean. Atmos. Chem. Phys. 20, 1839–1847. https://doi.org/10.5194/acp-20-1839-2020.

Sofiev, M., Ritenberga, O., Albertini, R., Arteta, J., Belmonte, J., Bonini, M., Celenk, S., Damialis, A., Douros, J., Elbern, H., Friese, E., Galan, C., Gilles, O., Hrga, I., Kouznetsov, R., Krajsek, K., Plu, M., Prank, M., Robertson, L., Steensen, B.M., Thibaudon, M., Segers, A., Stepanovich, B., Valdebenito, A.M., Vira, J., Vokou, D., 2017. Multi - model ensemble simulations of olive pollen distribution in Europe in 2014. Atmos. Chem. Phys. 17, 12341–12360. https://doi.org/10.5194/acp-17-12341-2017.

Sofiev, M., Siljamo, P., Ranta, H., Linkosalo, T., Jaeger, S., Rasmussen, A., Rantio-Lehtimaki, A., Severova, E., Kukkonen, J., 2012. A numerical model of birch pollen emission and dispersion in the atmosphere. Description of the emission module. Int. J. Biometeorol. 57, 54–58. https://doi.org/10.1007/s00484-012-0532-z.

Sofiev, M., Siljamo, P., Valkama, I., Ilvonen, M., Kukkonen, J., 2006. A dispersion modelling system SILAM and its evaluation against ETEX data. Atmos. Environ. 40, 674–685. https://doi.org/10.1016/j.atmosenv.2005.09.069.

Sofiev, M., Soares, J., Prank, M., de Leeuw, G., Kukkonen, J., 2011. A regional-to-global model of emission and transport of sea salt particles in the atmosphere. J. Geophys. Res. 116 https://doi.org/10.1029/2010JD014713.

Sofiev, M., Vira, J., Kouznetsov, R., Prank, M., Soares, J., Genikhovich, E., 2015b. Construction of an Eulerian atmospheric dispersion model based on the advection algorithm of M. Galperin: dynamic cores v.4 and 5 of SILAM v.5.5. Geosci. Model Dev. (GMD) 8, 3497–3522. https://doi.org/10.5194/gmd-8-3497-2015.

Tang, D., Wei, T., Yuan, J., Xia, H., Dou, X., 2021. The Transport of Bioaerosols Observed by Wideband Integrated Bioaerosol Sensor and Coherent Doppler Lidar (Preprint). Aerosols/Remote Sensing/Data Processing and Information Retrieval. https://doi.org/10.5194/amt-2021-401.

Tarasova, O.A., Brenninkmeijer, C.A.M., Assonov, S.S., Elansky, N.F., Roeckmann, T., Sofiev, M., 2007. Atmospheric CO along the Trans-Siberian railroad and river Ob: source identification using isotope analysis. J. Atmos. Chem. 57, 135–152. https://doi.org/10.1007/s10874-007-9066-x.

Thompson, L.R., Sanders, J.G., McDonald, D., Amir, A., Ladau, J., Locey, K.J., Prill, R.J., Gibbons, S.M., Ackermann, G., Navas-Molina, J.A., Janssen, S., Kopylova, E., Vázquez-Baeza, Y., González, A., Morton, J.T., Mirarab, S., Zech Xu, Z., Jiang, L., Haroon, M.F., Kanbar, J., Zhu, Q., Jin Song, S., Kosciolek, T., Bokulich, N.A., Lefler, J., Brislawn, C.J., Humphrey, G., Owens, S.M., Hampton-Marcell, J., Berg-Lyons, D., McKenzie, V., Fierer, N., Fuhrman, J.A., Clauset, A., Stevens, R.L., Shade, A., Pollard, K.S., Goodwin, K.D., Jansson, J.K., Gilbert, J.A., Knight, R., 2017. A communal catalogue reveals Earth's multiscale microbial diversity. Nature 551, 457–463. https://doi.org/10.1038/nature24621.

Thomsen, P.F., Willerslev, E., 2015. Environmental DNA – an emerging tool in conservation for monitoring past and present biodiversity. Biol. Conserv. 183, 4–18. https://doi.org/10.1016/j.biocon.2014.11.019.

Troudet, J., Grandcolas, P., Blin, A., Vignes-Lebbe, R., Legendre, F., 2017. Taxonomic bias in biodiversity data and societal preferences. Sci. Rep. 7, 9132. https://doi.org/10.1038/s41598-017-09084-6.

Tummon, F., Adamov, S., Clot, B., Crouzy, B., Gysel-Beer, M., Kawashima, S., Lieberherr, G., Manzano, J., Markey, E., Moallemi, A., O'Connor, D., 2021. A first evaluation of multiple automatic pollen monitors run in parallel. Aerobiologia. https://doi.org/10.1007/s10453-021-09729-0.

Valentini, A., Taberlet, P., Miaud, C., Civade, R., Herder, J., Thomsen, P.F., Bellemain, E., Besnard, A., Coissac, E., Boyer, F., Gaboriaud, C., Jean, P., Poulet, N., Roset, N., Copp, G.H., Geniez, P., Pont, D., Argillier, C., Baudoin, J.-M., Peroux, T., Crivelli, A. J., Olivier, A., Acqueberge, M., Le Brun, M., Møller, P.R., Willerslev, E., Dejean, T., 2016. Next-generation monitoring of aquatic biodiversity using environmental DNA metabarcoding. Mol. Ecol. 25, 929–942. https://doi.org/10.1111/mec.13428.

van Dijk, E.L., Jaszczyszyn, Y., Naquin, D., Thermes, C., 2018. The third revolution in sequencing technology. Trends Genet. 34, 666–681. https://doi.org/10.1016/j.tig.2018.05.008.

Van Goethem, M.W., Osborn, A.R., Bowen, B.P., Andeer, P.F., Swenson, T.L., Clum, A., Riley, R., He, G., Koriabine, M., Sandor, L., Yan, M., Daum, C.G., Yoshinaga, Y., Makhalanyane, T.P., Garcia-Pichel, F., Visel, A., Pennacchio, L.A., O'Malley, R.C., Northen, T.R., 2021. Long-read metagenomics of soil communities reveals phylum-specific secondary metabolite dynamics. Commun. Biol. 4, 1302. https://doi.org/10.1038/s42003-021-02809-4.

Veriankaitė, L., Siljamo, P., Sofiev, M., Sauliene, I., Kukkonen, J., 2010. Modelling analysis of source regions of long-range transported birch pollen that influences allergenic seasons in Lithuania. Aerobiologia 26, 47–62. https://doi.org/10.1007/s10453-009-9142-6.

Vesala, T., Järvi, L., Launiainen, S., Sogachev, A., Rannik, Ü., Mammarella, I., Ivola, E.S., Keronen, P., Rinne, J., Riikonen, A., Nikinmaa, E., 2008. Surface–atmosphere interactions over complex urban terrain in Helsinki, Finland. Tellus B 60, 188–199. https://doi.org/10.1111/j.1600-0889.2007.00312.x.

Vira, J., Sofiev, M., 2012. On variational data assimilation for estimating the model initial conditions and emission fluxes for short-term forecasting of SOx concentrations. Atmos. Environ. 46, 318–328. https://doi.org/10.1016/j.atmosenv.2011.09.066.

Woldringh, C.L., 1970. Lysis of the cell membrane of Escherichia coli K12 by ionic detergents. Biochim. Biophys. Acta Nucleic Acids Protein Synth. 224, 288–290. https://doi.org/10.1016/0005-2787(70)90650-7.

Wommack, K.E., Bhavsar, J., Ravel, J., 2008. Metagenomics: read length matters. Appl. Environ. Microbiol. 74, 1453–1463. https://doi.org/10.1128/AEM.02181-07.

Wood, D.E., Lu, J., Langmead, B., 2019. Improved metagenomic analysis with Kraken 2. Genome Biol. 20, 257. https://doi.org/10.1186/s13059-019-1891-0.

Wood, D.E., Salzberg, S.L., 2014. Kraken: ultrafast metagenomic sequence classification using exact alignments. Genome Biol. 15, R46. https://doi.org/10.1186/gb-2014-15-3-r46.

Xian, P., Reid, J.S., Hyer, E.J., Sampson, C.R., Rubin, J.I., Ades, M., Asencio, N., Basart, S., Benedetti, A., Bhattacharjee, P.S., Brooks, M.E., Colarco, P.R., da Silva, A. M., Eck, T.F., Guth, J., Jorba, O., Kouznetsov, R., Kipling, Z., Sofiev, M., Perez Garcia-Pando, C., Pradhan, Y., Tanaka, T., Wang, J., Westphal, D.L., Yumimoto, K.,

Zhang, J., 2019. Current state of the global operational aerosol multi-model ensemble: an update from the International Cooperative for Aerosol Prediction (ICAP). Q. J. R. Meteorol. Soc. 145, 176–209. https://doi.org/10.1002/qj.3497.

Yamamoto, N., Shendell, D.G., Peccia, J., 2011. Assessing allergenic fungi in house dust by floor wipe sampling and quantitative PCR: assessing house dust fungi by wipe sampling and qPCR. Indoor Air 21, 521–530. https://doi.org/10.1111/j.1600-0668.2011.00732.x.

Yooseph, S., Andrews-Pfannkoch, C., Tenney, A., McQuaid, J., Williamson, S., Thiagarajan, M., Brami, D., Zeigler-Allen, L., Hoffman, J., Goll, J.B., Fadrosh, D., Glass, J., Adams, M.D., Friedman, R., Venter, J.C., 2013. A metagenomic framework for the study of airborne microbial communities. PLoS One 8, e81862. https://doi.org/10.1371/journal.pone.0081862.

Yuan, H., Zhang, D., Shi, Y., Li, B., Yang, J., Yu, X., Chen, N., Kakikawa, M., 2017. Cell concentration, viability and culture composition of airborne bacteria during a dust event in Beijing. J. Environ. Sci. 55, 33–40. https://doi.org/10.1016/j.jes.2016.03.033.

Ziska, L., Knowlton, K., Rogers, C., Dalan, D., Tierney, N., Elder, M.A., Filley, W., Shropshire, J., Ford, L.B., Hedberg, C., Fleetwood, P., Hovanky, K.T., Kavanaugh, T., Fulford, G., Vrtis, R.F., Patz, J. a, Portnoy, J., Coates, F., Bielory, L., Frenz, D., 2011. Recent warming by latitude associated with increased length of ragweed pollen season in central North America. Proc. Natl. Acad. Sci. U. S. A 108, 4248–4251. https://doi.org/10.1073/pnas.1014107108.

Ziska, L.H., Makra, L., Harry, S.K., Bruffaerts, N., Hendrickx, M., Coates, F., Saarto, A., Thibaudon, M., Oliver, G., Damialis, A., Charalampopoulos, A., Vokou, D., Heiðmarsson, S., Guðjohnsen, E., Bonini, M., Oh, J.-W., Sullivan, K., Ford, L., Brooks, G.D., Myszkowska, D., Severova, E., Gehrig, R., Ramón, G.D., Beggs, P.J., Knowlton, K., Crimmins, A.R., 2019. Temperature-related changes in airborne allergenic pollen abundance and seasonality across the northern hemisphere: a retrospective data analysis. Lancet Planet. Health 3, e124–e131. https://doi.org/10.1016/S2542-5196(19)30015-4.